Neuroscience Institute Publications   Western Institute for Neuroscience

8-1-2022

Tonic pain alters functional connectivity of the descending pain modulatory network involving amygdala, periaqueductal gray, parabrachial nucleus and anterior cingulate cortex

Timothy J. Meeker
Johns Hopkins University

Anne Christine Schmid
Johns Hopkins University

Michael L. Keaser
University of Maryland Dental School

Shariq A. Khan
University of Maryland Dental School

Rao P. Gullapalli
University of Maryland School of Medicine

See next page for additional authors

Follow this and additional works at: https://ir.lib.uwo.ca/neurosci_inst_pubs

Authors

Timothy J. Meeker, Anne Christine Schmid, Michael L. Keaser, Shariq A. Khan, Rao P. Gullapalli, Susan G. Dorsey, Joel D. Greenspan, and David A. Seminowicz

Tonic pain alters functional connectivity of the descending pain modulatory network involving amygdala, periaqueductal gray, parabrachial nucleus and anterior cingulate cortex ☆

Timothy J. Meeker [a,b,c,*], Anne-Christine Schmid [a,b,c,d,e], Michael L. Keaser [b,c], Shariq A. Khan [b], Rao P. Gullapalli [f], Susan G. Dorsey [c,g], Joel D. Greenspan [b,c,1], David A. Seminowicz [b,c]

[a] Department of Neurosurgery, Johns Hopkins University, Baltimore, MD 21287, United States
[b] Department of Neural and Pain Sciences, University of Maryland School of Dentistry, Baltimore, MD 21201, United States
[c] Center to Advance Chronic Pain Research, University of Maryland Baltimore, Baltimore, MD 21201, United States
[d] Clinical Neuroengineering, BrainMind Institute and Centre of Neuroprosthetics (CNP), Swiss Federal Institute of Technology (EPFL) Geneva, Switzerland and Swiss Federal Institute of Technology Valais (EPFL Valais), Sion, Switzerland
[e] WyssCenter of Bio- and Neuroengineering, Geneva, Switzerland
[f] Department of Diagnostic Radiology and Nuclear Imaging, University of Maryland School of Medicine, Baltimore MD, 21201, United States
[g] Department of Pain and Translational Symptom Sciences, University of Maryland School of Nursing, Baltimore, MD 21201, United States

ARTICLE INFO

ABSTRACT

Introduction: Resting state functional connectivity (FC) is widely used to assess functional brain alterations in patients with chronic pain. However, reports of FC accompanying tonic pain in pain-free persons are rare. A network we term the Descending Pain Modulatory Network (DPMN) is implicated in healthy and pathologic pain modulation. Here, we evaluate the effect of tonic pain on FC of specific nodes of this network: anterior cingulate cortex (ACC), amygdala (AMYG), periaqueductal gray (PAG), and parabrachial nuclei (PBN).

Methods: In 50 pain-free participants (30F), we induced tonic pain using a capsaicin-heat pain model. functional MRI measured resting BOLD signal during pain-free rest with a 32 °C thermode and then tonic pain where participants experienced a previously warm temperature combined with capsaicin. We evaluated FC from ACC, AMYG, PAG, and PBN with correlation of self-report pain intensity during both states. We hypothesized tonic pain would diminish FC dyads within the DPMN.

Results: Of all hypothesized FC dyads, only PAG and subgenual ACC was weakly altered during pain ($F = 3.34$; $p = 0.074$; pain-free>pain $d = 0.25$). After pain induction sACC-PAG FC became positively correlated with pain intensity ($R = 0.38$; $t = 2.81$; $p = 0.007$). Right PBN-PAG FC during pain-free rest positively correlated with subsequently experienced pain ($R = 0.44$; $t = 3.43$; $p = 0.001$). During pain, this connection's FC was diminished (paired t=-3.17; $p = 0.0026$). In whole-brain analyses, during pain-free rest, FC between left AMYG and right superior parietal lobule and caudate nucleus were positively correlated with subsequent pain. During pain, FC between left AMYG and right inferior temporal gyrus negatively correlated with pain. Subsequent pain positively correlated with right AMYG FC with right claustrum; right primary visual cortex and right temporo-occipitoparietal junction

Conclusion: We demonstrate sACC-PAG tonic pain FC positively correlates with experienced pain and resting right PBN-PAG FC correlates with subsequent pain and is diminished during tonic pain. Finally, we reveal PAG- and right AMYG-anchored networks which correlate with subsequently experienced pain intensity. Our findings suggest specific connectivity patterns within the DPMN at rest are associated with subsequently experienced pain and modulated by tonic pain. These nodes and their functional modulation may reveal new therapeutic targets for neuromodulation or biomarkers to guide interventions.

1. Introduction

Functional connectivity (FC) has emerged over the past two decades as a technique to investigate the functional anatomy of human brain networks and the effects of psychological, pathological and perceptual manipulations, therapeutic treatments, and disease states on brain function (Baliki et al., 2012; Biswal et al., 1995; Crowther et al., 2015; Khalili-Mahani et al., 2017; Raichle et al., 2001). A network of brain regions, which we term the descending pain modulatory network (DPMN), has been well-studied during simultaneous experience of phasic painful heat stimuli, concurrent painful heat and distracting stimuli, during mind-wandering, placebo analgesia, and altered pain states such as brush allodynia (Becerra et al., 2006; Bingel et al., 2006; Eippert et al., 2009; Kucyi et al., 2013; Linnman et al., 2012b; Moulton et al., 2007; Petrovic et al., 2002; Valet et al., 2004). We consider a cortical or subcortical brain region to be part of the DPMN if it is differentially activated during pain modulation and has relatively high concentrations of μ-opioid receptors (Henriksen and Willoch, 2008). Demonstrating the potential clinical importance of the DPMN, enhanced FC within the DPMN during placebo analgesia and motor cortex stimulation is positively related to magnitude of analgesia experienced (Bingel et al., 2006; Eippert et al., 2009; Garcia-Larrea and Peyron, 2007; Meeker et al., 2019); additionally, there is a reduction of FC of the DPMN in chronic pain patients compared to pain-free controls (Linnman et al., 2012b; Yu et al., 2014). In healthy individuals, coactivation of the PAG and ACC during the experience of phasic pain coupled with analgesic cognitive manipulations, such as placebo, results in enhanced FC between these regions accompanied by a reduction in perceived pain intensity (Bingel et al., 2006; Eippert et al., 2009; Fairhurst et al., 2007; Kucyi et al., 2013; Sprenger et al., 2011; Valet et al., 2004). Several regions in the ACC surrounding the genu of the corpus callosum have been implicated in pain modulation, therefore we interrogate three separate ROIs in the region of the ACC including pregenual (pACC), anterior subgenual ACC (sACC) and supragenual ACC (spACC) (Bingel et al., 2006; deCharms et al., 2005; Seymour et al., 2005; Valet et al., 2004; Wiech et al., 2005).

While several studies have evaluated the network's FC during phasic painful stimuli there is a scarcity of studies exploring FC during prolonged tonic pain (Ayoub et al., 2021; Bingel et al., 2006; Kucyi et al., 2013; Seminowicz and Davis, 2007; Valet et al., 2004). Tonic pain states, such as those encountered in chronic pain syndromes, display unique perceptual dynamics and modeling prolonged tonic pain in healthy participants is a critical intermediate step in understanding the neurophysiology of chronic pain disorders (Baliki et al., 2006; Foss et al., 2006).

To probe the functional modulation of relationships within the DPMN during a prolonged tonic painful stimulus in a preclinical human pain model, we acquired resting state fMRI scans in pain-free participants before and after exposing them to a potent topical capsaicin-heat pain (C-HP) model (Anderson et al., 2002; Meeker et al., 2019), thereby capturing pain-free and prolonged tonic pain resting states within a single imaging session.

In this report, we predicted that prolonged tonic pain would disrupt the coupling between the ACC and PAG since disruption in FC between ACC and PAG occurs in chronic pain disorders and the ACC displays reductions in local FC in chronic pain (Ke et al., 2015; Khalili-Mahani et al., 2017; Li et al., 2016; Liu et al., 2012; Wei et al., 2016; Wu et al., 2016). We further predicted enhanced FC between the AMYG and PBN during tonic pain compared to the pain-free state given the amygdaloparabrachial transmission pathway and its role in pain response and modulation as evidenced in rodent studies (Chen and Heinricher, 2019; Kissiwaa and Bagley, 2018; Raver et al., 2020; Roeder et al., 2016; Uddin et al., 2018). Finally, we predicted modulation of a functional connection between the PAG and parabrachial nucleus, given primate tractography and rodent neurophysiology implicating this pathway in pain modulation (Chen and Heinricher, 2019; Mantyh, 1982a, 1983; Roeder et al., 2016). Support for these predic-

tions would add to the growing body of evidence of the association of the DPMN to the perception of tonic pain in healthy humans.

2. Methods

2.1. Overview

We report results from a total of 50 participants enrolled in one of two studies conducted at University of Maryland Baltimore (UMB) from October 2011 until December 2015. Study 1 set out to establish the effects of a prolonged tonic pain stimulus lasting several minutes on the functional organization of the human brain (Fig. 1A). In the first study, we conducted experiments provoking pain in 18 healthy participants (10 M; 2 left-handed) aged 23 to 61 (median=30.5) by applying 10% capsaicin cream under a warm thermode on their left leg, which we term the capsaicin-heat pain (C-HP) model to distinguish it from previous models using lower concentration capsaicin creams (Anderson et al., 2002; Cavallone et al., 2013; Meeker et al., 2019; Petersen and Rowbotham, 1999). We conducted a screening session to eliminate participants who did not develop sufficient heat allodynia during the C-HP (Liu et al., 1998). Eligible participants then took part in an MRI session which was separated by ≥13 days (median=39.5 (range=13 to 88)) from the screening session. Using the C-HP model we maintained a mild to moderate pain intensity with a 39 °C ($n = 11$), 40 °C (6) or 41 °C (1) thermode. The temperature selected for each participant was based on that individual's thermal heat pain sensitivity evaluated at screening just prior to the C-HP exposure.

In study 2, 40 participants (17 M; median age: 24; range 20–39) underwent an MRI in which we employed the C-HP model with a 38 °C ($n = 4$), 39 °C (2), 40 °C (6), 41 °C (8), or 42 °C (20) thermode (Fig. 1B). From this group of participants, 3 males were excluded from the current report because they reported pain ratings of 0 out of 100 during the last 2 min of exposure to the C-HP model (C-HP temperatures for these participants were all 42 °C). A further 4 males and 1 female were excluded due to having greater than 0.5 mm motion framewise displacement in at least 10% of the functional MR time series (1 at 40 °C, 1 at 41 °C, 2 at 42 °C). Resting state fMRI results from study 1 and 2 are pooled together and use the same MRI sequence and protocol, excepting that scans were acquired at different resolutions ($1.8 \times 1.8 \times 4$ mm³ versus 3 mm³ isotropic) with different head coils (12- versus 32- channel). All participants provided written informed consent, and all procedures were approved by the UMB Institutional Review Board for the Protection of Human Subjects.

2.1.1. Eligibility criteria

In study 1 exclusion criteria were: pregnancy; history of brain injury with any period of unconsciousness; illicit, or prescription opioid, drug use; current pain or history of chronic pain; history of cardiac, renal, hepatic, or pulmonary function disorders; history of cancer; ambidextrous (Oldfield, 1971); hospitalized for a psychiatric disorder within last 12 months; pain intensity rating less than 21 on a 0–100 NRS while exposed to the C-HP model. Illicit drug use was determined with a urine drug screen for marijuana, cocaine methamphetamine, amphetamines, ecstasy, heroin, phencyclidine, benzodiazepines, methadone, barbiturates, tricyclic antidepressants or oxycodone (First Check™).

In study 2, in addition to eligibility criteria for study 1, we excluded left-handed participants, any individual with any diagnosis of psychological or neurological disorder or participants taking any psychoactive medications (by self-report). However, in study 2 we did not exclude any individual based on sensitivity to the C-HP model.

2.1.2. Psychophysics and psychological questionnaires

During the initial session of each study, we measured participants' warmth detection thresholds (WDTs) and heat pain thresholds (HPTs) with a Medoc stimulator (Pathway; Medoc; Ramat Yishai, Israel) using
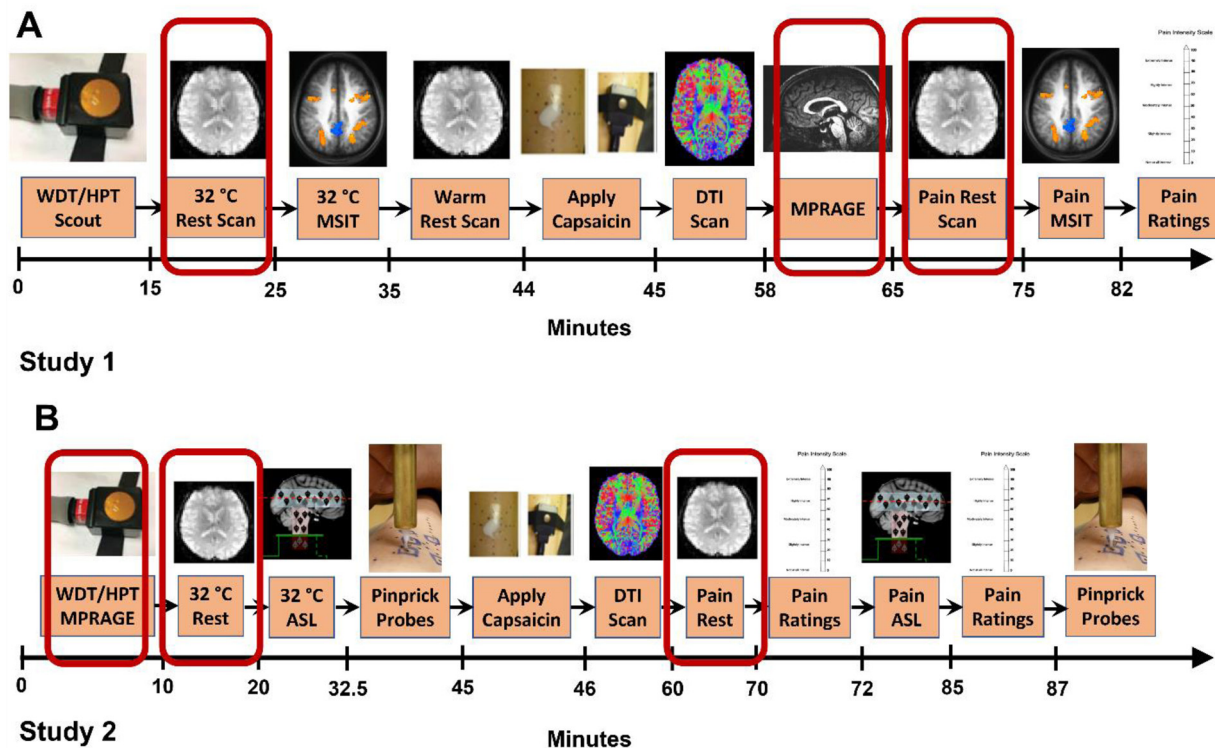
Fig. 1. (A) In study 1, 18 participants experienced a pain-free resting state scan and 40 min later experienced the same resting state scan while experiencing thermal allodynia induced by capsaicin. (B) In study 2, 40 participants experienced a pain-free resting state scan and then 40 min later experienced the same resting state scan while experiencing thermal allodynia induced by capsaicin. Scans used in the analysis in the present report are demarcated in red. Abbreviations: WDT – warmth detection threshold; HPT – heat pain threshold; MSIT – multi-source interference task (Bush and Shin, 2006); DTI – diffusion tensor imaging; ASL – arterial spin label; MPRAGE – magnetization prepared rapid acquisition gradient echo. (For interpretation of the references to color in this figure legend, the reader is referred to the web version of this article).

the method of limits (Greenspan, 2013). We placed the 3×3 cm contact area stimulator on the lower left foreleg at a baseline temperature of 32 °C. A program increased the temperature at a ramp of 0.5 °C/s until the participant pressed a mouse button. We instructed the participant to press the button when they "felt a change in temperature" for WDTs or when the warmth "becomes painful" for HPTs. At a single site, we measured four trials for WDTs and HPTs. We took the average of the last three threshold determinations for each participant. In study 2, the protocol for HPTs started with a baseline of 30 °C, to accommodate sensitivity changes after capsaicin exposure.

2.1.3. Capsaicin-heat pain model

To produce a safe, sustained painful experience, we treated participant's lower left foreleg with one gram of 10% capsaicin cream under a Tegaderm™ bandage (Anderson et al., 2002; Meeker et al., 2019). To control the exposure area, we applied the cream within a 2.5 cm² square cut into a Tegaderm™ bandage. After 12 min of exposure – long enough for the capsaicin cream to reach saturating concentrations at the intraepidermal nerve fiber endings – we placed the thermode over the topmost bandage at the designated temperature (Green and Flammer, 1988). During study 2 the incubation period was increased to 15 min and the thermode was placed on the participant's leg during incubation, held at 32 °C. Target temperatures used were tailored for each participant between the pre-capsaicin WDT and HPT. Participants rated pain intensity on a numerical rating scale (NRS) with verbal anchors on one side, and numbers ranging from 0 to 100 in increments of 10 (Greenspan et al., 2003). In study 1, participants provided pain intensity ratings every 30 s for 10 min after application of the thermode. Participants reporting average NRS pain 30 out of 100, and tolerating the C-HP model, were eligible for MRI sessions. During study 2 participants provided pain intensity ratings every minute for 35 min during the entire

capsaicin exposure. At the end of the exposure period, we removed the bandages and capsaicin with an isopropanol swab. This C-HP procedure does not cause tissue damage (Moritz and Henriques, 1947). After each exposure to the C-HP model, participants filled out several psychological questionnaires including the short-form McGill Pain Questionnaire, version 2 (SF-MPQ-2) (Dworkin et al., 2009). This questionnaire is generally used in chronic pain populations to provide some characterization of patients' pain experience. For this study, we modified the SF-MPQ-2 to change the instructions from '… pain and related symptoms you felt during the last week' to '… pain and related symptoms you felt during today's pain experience.' We include comprehensive results of this questionnaire from participants who completed the form after their MRI scanning session ($n = 36$). Validity of the original MPQ in experimental pain has been explored and supported by previous studies (Chen and Treede, 1985; Crockett et al., 1977; Klepac et al., 1981; Koenig et al., 2014). The use of multiple versions of the MPQ including the SF-MPQ has been reported in both pain models and for evaluation of the qualities of different modalities of phasic pain in pain-free health participants (Harrison and Davis, 1999; Mischkowski et al., 2021; Price et al., 2018; Stohler and Kowalski, 1999; Strigo et al., 2002; Walsh et al., 1995).

2.1.4. MRI procedures

We recorded fMRI in a 3-T Tim Trio scanner (Siemens Medical Solutions, Malvern, PA) using a 12-channel (study 1) or 32-channel (study 2) head coil with parallel imaging capability. For resting state scans during study 1, we used a gradient echo single-shot echo-planar-imaging (EPI) sequence with 30 ms echo time (TE), 90° flip angle and 2500 ms repetition time (TR) providing T2*-weighted volumes in 36 interleaved, 4 mm slices (no gap) with an in-plane resolution of 1.8 mm². For study 2, we used identical parameters except that we collected 44 interleaved, 3 mm slices (no gap) with an in-plane resolution of 3.0 mm². During both rest-

ing state scans participants fixated on a crosshair for 8 min 12.5 s providing 194 functional volumes. For anatomical reference, we acquired a 3-dimensional T1 magnetization-prepared rapid gradient echo (MPRAGE) volumetric scan with 2.9 ms TE, 2300 ms TR, 900 ms inversion time (TI), flip angle 9°, 144 slices, axial slice thickness 1.0 mm and 0.9 mm² in-plane resolution over a 23-cm field of view for 13 of 18 participants belonging to study 1. The remaining participants from study 1 and all participants from study 2 received a modified MPRAGE acquisition which facilitated isotropic resolution and provided extended coverage of the brain: 2.9 ms TE, 2300 ms TR, 900 ms TI, flip angle 9°, 176 slices, sagittal slice thickness 1.0 mm and 1.0 mm² in-plane resolution over a 25.6-cm field of view. Since structural scans were used for anatomical reference and display only, this difference in anatomical acquisition did not influence the results.

2.1.5. fMRI session protocol

During study 1 and 2 MRI sessions, we evaluated the participants' WDTs and HPTs in the MRI environment. During the resting state scan participants were told: "Please stare at the plus sign, do not move and do not fall asleep. You may let your mind wander." Then, we increased the thermode temperature to the predetermined target, while the participant fixated on the cross hair for the duration of the scan. After the scan, participants remained in the scanner with the thermode in place and rated their pain intensity every 30 s for two minutes on a 0–100 NRS. In study 1, the control resting state was always before the pain resting state scan and the two were a median of 45.5 min apart (Range: 45 to 50 min), while the pain ratings were taken a median of 7 min (Range: 7 to 10 min) from the end of the pain resting state scan (Fig. 1A). In study 2, the control resting state was also always before the pain resting state scan and the two were a median of 48 min apart (Range: 44 to 64 min), while pain ratings were immediately after the pain resting state scan (Fig. 1B).

2.1.6. Statistical methods

Effects of time on sensory detection thresholds (WDTs and HPTs), after exposure to the C-HP model, were evaluated using a linear mixed model (LMM) with time as a fixed factor and participant as a random factor. In different models, either baseline HPT or baseline WDT were using as a control to compare to HPTs taken at 25, 50 and 75 min after capsaicin removal. Multiple comparisons were corrected using Tukey's HSD. The R package 'anova' was used to derive F-stats for the overall model. We conducted this set of statistical tests using R 3.4.1.

2.1.7. Resting state fMRI data analysis

All preprocessing of resting state fMRI scans used the afni_proc.py python script for Analysis for Functional NeuroImaging (AFNI) version 27 Jun 2019. The first three volumes were automatically removed from the functional scan series by the MRI scanner to allow for signal equilibration. We used 3dToutcount to determine the minimum outlier EPI volume for later EPI volume registration and alignment. Outliers were defined in relation to the median absolute deviation of the signal time course (see afni.nimh.nih.gov/pub/dist/doc/program_help/3dToutcount.html for outlier definition). Each functional time series was detrended and spikes quashed with 3dDespike. Then, each volume was slice-time corrected and aligned to the first slice collected during the TR. Before aligning the anatomical scan to the functional scan, the skull was removed from each individual Freesurfer processed anatomy using 3dSkullStrip. We used 3dAllineate via the align_epi_anat.py python script to align the anatomy to the minimum outlier functional EPI volume using the local Pearson correlation signed cost functional while allowing different cost functionals for initial alignment if, for example, alignment fails (e.g., lpc+ZZ). After alignment, the anatomical volume was warped to MNI atlas space and normalized to the MNI152, version 2009, skull-stripped brain using @auto_tlrc. Each EPI volume was then registered to the base, minimum outlier, EPI volume. Then, the registered EPI volumes were aligned to the template-aligned structural

volume using non-linear warping. Following this final functional alignment, a full alignment matrix was estimated and applied to the anatomy follower dataset from Freesurfer including default Freesurfer parcellations (e.g., aaseg) and ventricle and white matter segments, which were first eroded by 1 mm³. Since the DPMN, as we have defined it, involves several midbrain and brainstem regions, each 4D EPI dataset was then blurred with a 4 mm FWHM Gaussian spatial filter. To provide a normalized across participant standard interpretation of signal fluctuations and prevent any participant from outweighing any other participant, we scaled the 4D BOLD signal to a normalized value of a mean of 100 and range from 0 to 200.

In the participant-level regression model regressors of no interest included a binary regressor excluding volumes with motion exceeding 0.5 mm in framewise displacement, the principal component of signal extracted from the individual eroded Freesurfer ventricle masks, demeaned motion parameters (motion in x, y and z planes and rotation about the x, y and z axes), and their first order derivatives. There were 72 out of 9700 (0.74%) volumes censored during the pain-free resting state scan and 118 out of 9700 (1.22%) volumes censored during the pain state scan. We did not regress out any signal or signal-derivative from white matter, since using white matter masks derived from Freesurfer segmentation removed through partial volume effects and mismatching of voxel geometry between MPRAGE and T2* images, variance from gray matter in the cortex as well as brainstem. Recent evidence of signal of interest related to gray matter BOLD signal exists in the white matter further supports our approach (Li et al., 2020b; Mishra et al., 2020; Peer et al., 2017; Vos de Wael et al., 2017). However, in consideration of the literature supporting WM regression resting state FC analysis, we present results of the primary analyses after afni's ANATICOR WM regression with freesurfer WM masks eroded by 5 mm (Supplemental Figs. 1–3) (Bartoň et al., 2019; Jo et al., 2010; Vos de Wael et al., 2017). An LMM of average head motion measured as framewise displacement for each participant with factors of sex and state found no significant effect of state ($F = 1.99$; $p = 0.165$), sex ($F = 0.75$; $p = 0.389$), or state-by-sex interaction ($F = 2.32$; $p = 0.134$). Pain intensity during the pain state was not related to average framewise displacement during the pain-free ($R=-0.031$; $t=-0.22$; $p = 0.83$) or pain state scan ($R = 0.031$; $t = 0.22$; $p = 0.83$). For each participant, the regressor of interest was the seed time course for that specific seed and session. We have divided our report into cortical, subneocortical and basal ganglia regions of interest. Here we report the results of the subneocortical investigation including the periaqueductal gray (PAG), left and right AMYG and left and right parabrachial regions. We exclude the dorsal raphe and rostral ventromedial medulla as seeds as specific fMRI acquisition methods are recommended to optimize acquisition of signal from the medulla (Beissner et al., 2014; Stroman et al., 2018). The seed regions of interest were left and right AMYG as defined by Freesurfer parcellation, three bilateral 5 mm radius ROIs in the anterior cingulate cortex corresponding to supragenual (MNI: ±6, (median=35; min=33; max=37), (median=12; min=10; max=14)), pregenual (MNI: ±6, (median=38; min=37; max=40), (median=1; min=−2; max=3)) and subgenual (MNI: ±5, (median=31; min=29; max=37), (median=−9; min=−11; max=−7)) ACC, and 3 mm radius spheres for left and right parabrachial nucleus (PBN) in (MNI: $x=\pm10$, $y=-35$, $z=-30$), and a participant-specific anatomically drawn seed for the PAG (PAG; group average center of mass: MNI: (0, −29, −10)) (Fairhurst et al., 2007; Linnman et al., 2012b; Morey et al., 2009; Sprenger et al., 2011). The PAG seed was drawn to encompass all apparent gray matter surrounding the cerebral aqueduct on T1 MPRAGE images after alignment into atlas space. ACC seeds were placed on individual participant anatomies and tests completed to ensure they did not overlap and were placed within gray matter. Seeds that were drawn or placed anatomically by TJM (L- and RPBN, spACC, pACC, sACC and PAG) were each reviewed for placement by both TJM and JDG on individually aligned anatomical images. Since few reports of network brain connectivity in humans including the whole brain have reported FC in the context of tonic pain in

otherwise healthy participants, we include exploratory analysis of each seed region including contrasts and with FC covariation with pain intensity experienced during tonic pain (Ayoub et al., 2021; Pritchard et al., 2000; Stroman et al., 2018).

Seed-to-seed FC analysis was performed on the R-to-Z-transformed FC of the following dyads: spACC-PAG, pACC-PAG, sACC-PAG, spACC-left amygdala (LAMYG), spACC-right amygdala (RAMYG), pACC-LAMYG, pACC-RAMYG, sACC-LAMYG, sACC-RAMYG, sACC-LPBN, sACC-RPBN, LPBN-LAMYG, RPBN-RAMYG, LPBN-PAG, and RPBN-PAG. Each LMM included participant as a random effects factor, and state (tonic pain vs. pain-free), sex (M vs. F) and study (Study 1 vs. Study 2) as fixed effects factor. We included sex as a factor in our model since prior research has reported significant sex differences in functional connectivity in healthy participants in brain-wide analyses from the PAG and sACC (Linnman et al., 2012a; Wang et al., 2014). We included study as a factor, given the differences in our study 1 and 2 scanner equipment, and the necessity to pool the 50 participants in a simple paired t-test to achieve an estimated power of 0.8 with an effect size of $d = 0.4$. Sample size determination for LMMs is not yet a settled question given the flexibility of the models. We used the R package lmer and lmerTest to 1) generate the 8 possible LMMs of interest including state and 2) compare these models to the intercept model and to each other to select the 'best' model for each dyad. We additionally confirmed our model selection using the R function 'step.' In 3 of 15 cases the step function found the maximal model (~1+State*Sex*Study) as the best model, which model comparison determined to be overfit in each case. We calculated realized power given found effect sizes and sample size using the R package 'pwr.' Finally, for trending or significant contrasts of sex or state, we report effect sizes calculated using the t-stat and sample size from the LMM summary report (Lakens, 2013). We assessed the effects of WM regression on dyad analysis using an LMM by extracting signal from the same ROIs after 4 different levels of WM regression: no WM regression, WM regression after 1 mm mask erosion, WM regression after 3 mm mask erosion, and WM regression after 5 mm mask erosion. The effect of WM mask erosion was significant for the RPBN-PAG ($F = 2.71$; $p = 0.045$) and spACC-LAmyg ($F = 4.70$; $p = 0.0031$), where neither state nor study factors were significant (Supplemental Table 1). Specifically for these dyads, supported by extensive evidence from functional and tract-tracing animal models and prior structural and functional connectivity findings in healthy and chronic pain participants or functional coupling reactive to nociceptive stimuli in animal models, we assessed significance at each test at $p<0.05$ (Supplemental Table 2). It should be noted the guidelines 'significance' of p-values, are arbitrary and participant to test assumptions, sample size, context, and practical effect interpretation (Fisher, 1948; Wasserstein and Lazar, 2016). Degrees of freedom for F-tests and posthoc analyses were corrected using the Satterthwaite correction (Luke, 2017). Additionally, we calculated Pearson correlation between across group, Z-normalized, mean-centered pain intensity scores during the tonic pain state with each FC dyad for each state. We report both uncorrected p-values and if they are significant after Bonferroni correction for the 30 dyad-state pairings and 15 contrasts between states for each dyad, as a subtraction of t-stats of the R-scores calculated on each dyad. This analysis was completed with R version 3.6.3.

2.1.8. Group level whole-brain fMRI analysis

For group level analysis, we used AFNI's linear mixed-effects modeling program 3dLME (Chen et al., 2013). A two-factor model focused on the change in state between the pain-free and prolonged tonic pain resting states with the C-HP model inducing heat allodynia (factor levels: pain-free and tonic pain) to arrive at tonic pain - pain-free contrast maps and mean seed-driven functional connectivity network (FCN) maps. For pain intensity covariation with seed-driven, FC we used AFNI's 3dttest++. All analyses were restricted within a group gray matter probability mask which excluded ventricles and cortical white matter regions. First each individual gray matter mask was created by subtract-

ing the individual binary Freesurfer ventricle and cortical white matter masks from the group union functional mask. Then the group binary gray matter probability mask was created by including voxels where at least 30 of 50 individual participants had gray matter For FCN maps of brainstem and midbrain seeds we cluster-extent corrected for R-score and p-value, thresholding at $R = 0.10$ and $p = 0.0001$. For FCN maps of amygdala seeds we cluster-extent corrected for R-score and p-value, thresholding at $R = 0.20$ and $p = 0.0001$. To correct for multiple comparisons, we estimated the spatial autocorrelation function of the residual noise of the BOLD signal within our analysis mask using 3dFWHMx and used the resulting parameters with 3dClustSim to calculate cluster extent criteria (CEC) for both 3dLME and 3dttest++ resultant maps.

We implemented an initial voxel-wise threshold of 0.001, with a cluster-extent correction of 270 mm³. To elucidate the coordinates of local maxima within large clusters, we iteratively reevaluated statistical maps after reducing the p-value threshold of each map by a factor of 10 (e.g., 0.001–0.0001). This process was completed by hand after generating all possible iterative voxel tables using 3dclust. For group FCN maps voxel tables, we implemented an initial minimum cluster-extent corrected for R-score and p-value, thresholding at $R = 0.10$ ($R = 0.20$ for AMYG seeds) and $p = 0.0001$. We followed a similar iterative process for FCN voxel tables as for contrast and covariate voxel tables but increased the R-score in 0.05 steps.

3. Results

3.1. Psychophysical and perceptual response to capsaicin-heat pain (C-HP) model during screening session

All participants included in this analysis reported hot-burning pain in response to the C-HP model. For participants in study 2 ($n = 32$), the time course for pain intensity ratings during the screening session shows an ever-increasing trend during the C-HP exposure, which responded positively to 0.5 °C step increases at each arrow (Fig. 2A). The thermode temperature for the MRI scan was tailored for each participant, and once increased to the target temperature, remained stable during the MRI sessions. Further, in study 2 ($n = 32$), exposure to the C-HP model induced profound heat allodynia which lasted at least 75 min after capsaicin removal ($F = 11.28$; $p<0.001$) (Fig. 2B). HPTs after capsaicin removal were all significantly lower than pre-capsaicin exposure HPTs ($t\leq -7.8$; $p \leq 10^{-8}$) and the first HPTs after C-HP removal were lower than baseline WDTs ($t=-4.5$; $p = 8.4 \times 10^{-5}$), demonstrating profound hypersensitivity to heat after C-HP exposure. Using SF-MPQ-2 descriptors, most participants described the pain as throbbing, aching, heavy, tender, shooting, stabbing, sharp, piercing, sensitive to touch, hot-burning and tingling (Fig. 2C). After removing the descriptor 'hot-burning' from the analysis, we found a significant effect of pain descriptor class ($F = 9.17$; $p<0.0001$) and no effect of sex on participants' ratings on the SF-MPQ-2 ($F = 0.18$; $p = 0.67$). Participants rated both intermittent and continuous pain descriptors higher than either neuropathic or affective pain descriptors (Continuous>Affective: $t = 4.0$; $p<0.001$; Intermittent>Affective: $t = 4.0$; $p<0.001$; Continuous>Neuropathic: $t = 4.1$; $p<0.001$; Intermittent>Neuropathic: $t = 4.1$; $p<0.001$). There was no difference in ratings between continuous and intermittent descriptors, and neuropathic and affective descriptors ($t<0.13$; $p>0.98$). During the MRI experiment, during the two minutes immediately after the corresponding tonic pain resting state scan average pain intensity of the group was rated as 33 (SD=21) on a 0–100 point scale with a range of 1–75.

3.2. Seed-to-Seed hypothesized resting state functional connectivity modulation: effects of tonic pain on specific DPMN dyads

For the LMM analysis including sex, state and study as factors, connectivity of the three ACC seeds to the PAG, only sex was a significant factor for the pACC-PAG connection ($F = 4.07$; $p = 0.049$; $M>F$
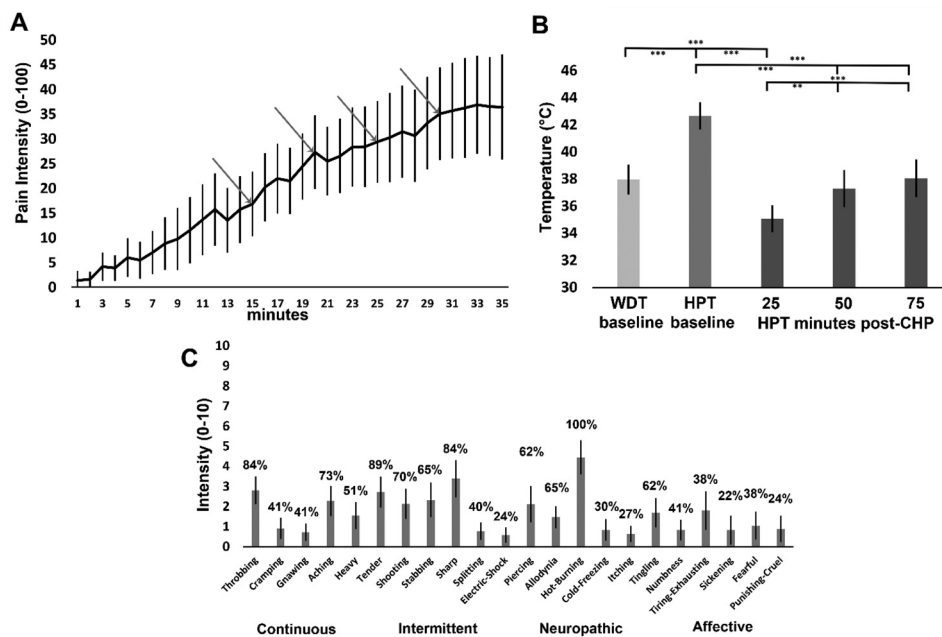
Fig. 2. (A) Ratings of prolonged tonic pain intensity during C-HP, the first arrow is when the thermode increased to the target temperature and the temperature increased 0.5 °C at each subsequent arrow ($n = 32$). (B) Warmth detection thresholds (WDT) and heat pain thresholds (HPT) taken before and after exposure to the C–HP model ($n = 32$); ** - $p = 0.0002$; *** - $p < 0.0001$. (C) Mean intensity of pain descriptors from the SF-MPQ-2, where percentages above each bar represent percentage of participants endorsing pain descriptor with any non-zero rating ($n = 36$). Error bars are 95% confidence intervals.

Table 1
Correlation between functional connectivity strength and pain intensity.

Functional Connectivity Dyad	State	R-score	t-stat	p-value
1. L-PBN to left amygdala	Pain-free	−0.0087	0.06	0.95
2. L-PBN to left amygdala	Pain	0.020	0.14	0.89
3. R-PBN to right amygdala	Pain-free	0.236	1.68	0.099
4. R-PBN to right amygdala	Pain	0.0088	0.06	0.95
5. pACC to left amygdala	Pain-free	0.152	1.07	0.29
6. pACC to left amygdala	Pain	−0.0836	−0.581	0.56
7. pACC to right amygdala	Pain-free	0.0302	0.209	0.84
8. pACC to right amygdala	Pain	−0.0976	−0.679	0.50
9. sACC to left amygdala	Pain-free	−0.0551	−0.382	0.70
10. sACC to left amygdala	Pain	−0.0146	−0.101	0.92
11. sACC to right amygdala	Pain-free	−0.133	−0.93	0.36
12. sACC to right amygdala	Pain	−0.0316	−0.22	0.83
13. spACC to left amygdala	Pain-free	0.0840	0.58	0.56
14. spACC to left amygdala	Pain	−0.190	−1.34	0.19
15. spACC to right amygdala	Pain-free	0.116	0.81	0.42
16. spACC to right amygdala	Pain	−0.174	−1.22	0.23
17. L-PBN to PAG	*Pain-free*	*0.341*	*2.51*	*0.016*
18. L-PBN to PAG	Pain	0.180	1.27	0.21
19. R-PBN to PAG	**Pain-free**	**0.444**	**3.43**	**0.001**
20. R-PBN to PAG	Pain	0.0375	0.26	0.80
21. sACC to L-PBN	Pain-free	−0.271	−1.95	0.057
22. sACC to L-PBN	Pain	0.114	0.79	0.43
23. sACC to R-PBN	Pain-free	−0.0828	−0.58	0.57
24. sACC to R-PBN	Pain	−0.0133	−0.09	0.93
25. pACC to PAG	Pain-free	0.174	1.22	0.23
26. pACC to PAG	Pain	0.0641	0.45	0.66
27. sACC to PAG	Pain-free	0.0618	0.43	0.67
28. sACC to PAG	*Pain*	*0.376*	*2.81*	*0.007*
29. spACC to PAG	Pain-free	0.229	1.63	0.11
30. spACC to PAG	Pain	0.0663	0.46	0.65

italics - significant before BF correction. BOLD - significant after BF correction.

Cohen's $d = 0.40$), while the state factor for sACC-PAG did not surpass our threshold for significance ($F = 3.13$; $p = 0.083$; pain-free>pain $d = 0.25$) (Table 1). State was also not significant for either the pACC-PAG ($F = 0.66$; $p = 0.42$) or spACC-PAG ($F = 2.63$; $p = 0.11$) connections. No LMM with any factor was significant compared to the null (intercept) model for the sACC to LPBN or sACC to RPBN connections indicating no factors were significant (Table 1).

For the four connections from the left and right PBN, the effect of state was significant for the RPBN to PAG connection indicating stronger FC during pain compared to the pain-free state ($F = 4.33$; $p = 0.043$;

$d = 0.294$) in the model including study ($F = 1.76$; $p = 0.19$) and the interaction of study and state ($F = 8.01$; $p = 0.0068$). For the remaining connections from PBN evaluated, no LMM with any factor was significant compared to the null (intercept) model for the LPBN to PAG, LPBN to LAMYG or RPBN to RAMYG connections indicating no factors were significant (Table 1).

For the spACC to LAMYG connection, sex was a significant factor with stronger FC in males compared to females ($F = 4.81$; $p = 0.033$; $d = 0.310$). While state produced no significant effects on any of the six functional connections from the ACC to left or right amygdala, there were some trends in state changes. Specifically, both the spACC to RAMYG ($F = 3.26$; $p = 0.077$; $d = 0.255$) and sACC to RAMYG connections ($F = 3.16$; $p = 0.082$; $d = 0.251$) trended stronger during pain compared to the pain-free state. For the remaining connections from the amygdala evaluated, no LMM with any factor was significant compared to the null (intercept) model for the pACC to LAMYG, pACC to RAMYG or sACC to LAMYG connections indicating no factors were significant (Table 1).

We tested for correlations of pain intensity during the tonic pain experience for with each FC dyad during both the pain and pain-free states (Table 1). Before induction of the tonic pain model correlation between pain intensity and FC between the sACC and PAG was not significant, however, during the tonic pain experience correlation between pain intensity and FC between the sACC and PAG became positive ($R = 0.38$; $t = 2.81$; $p = 0.007$) (Fig. 3A), but did not survive after BF correction (over 30 dyads). Furthermore, the change in correlation between pain intensity and FC of sACC and PAG between pain and pain-free states was significant ($t = 2.38$; $p = 0.021$), but did not survive BF correction. Before induction of tonic pain, pain intensity of subsequently experienced pain was positively correlated with the FC of LPBN and PAG ($R = 0.34$; $t = 2.51$; $p = 0.016$) (before BF correction), but this FC correlation with pain intensity measured during the tonic pain experience was not significant. The change between states did not significantly change the relationship between the FC of LPBN and PAG and pain intensity ($t = 1.24$; $p = 0.22$). Before induction of tonic pain, pain intensity of subsequently experienced pain was positively correlated with the FC of RPBN and PAG ($R = 0.44$; $t = 3.43$; $p = 0.001$), but FC measured during the tonic pain experience was not significant (Fig. 3B). The change between states significantly changed the relationship between the FC of RPBN and PAG and pain intensity ($t=−3.17$; $p = 0.0026$), surviving BF correction (15 possible changes in FC-pain intensity correlation).
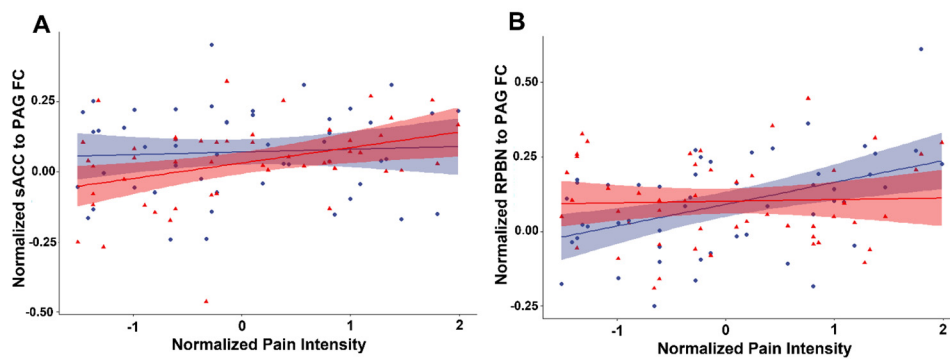
Fig. 3. (A) Correlation between normalized pain intensity and functional connectivity between subgenual anterior cingulate cortex and periaqueductal gray during the pain-free (blue circles) and tonic pain states (red triangles). (B) Correlation between normalized pain intensity and functional connectivity between right parabrachial nucleus and periaqueductal gray during the pain-free (blue circles) and tonic pain states (red triangles). Shaded areas correspond to 95 percent confidence bounds. (For interpretation of the references to color in this figure legend, the reader is referred to the web version of this article.).

3.3. Resting state functional connectivity: seed-driven networks during pain-free and prolonged tonic pain states

Seed-driven FC from the LPBN ($R > 0.12$) during the resting state scan with a 32 °C thermode on the participant's leg (hereafter, 'pain-free state') demonstrated significant BOLD signal correlation subcortically with the left ventral striatum, left medial dorsal region of the thalamus and right caudate nucleus (Supplemental Fig. 4A and Supplemental Table 3). LPBN showed cortical FC with the left anterior midcingulate cortex (aMCC), right lingual gyrus, right medial precuneus and left parietal-occipital sulcus. After induction of heat allodynia during the tonic pain state, LPBN whole brain FC was greater on average and showed additional regions of FC ($R > 0.12$). Additional regions of FC with LPBN included left postcentral gyrus, left ventral anterior insula, right dorsal posterior insula, bilateral inferior frontal gyri and bilateral lateral PAG (Supplemental Fig. 4B and Supplemental Table 4).

Seed-driven FC from the RPBN ($R > 0.12$) during the pain-free state included subcortical regions including the contralateral LPBN, midline rostral pons, right caudate nucleus, right substantia nigra, bilateral ventral striatum, bilateral cerebellar tonsil, and left thalamus including the lateral geniculate nucleus and pulvinar (Supplemental Fig. 5A and Supplemental Table 5). Pain-free state FC from the RPBN to cortical regions including left fusiform gyrus, left precentral gyrus, left middle frontal gyrus, left middle temporal gyrus, right cuneus, right inferior frontal gyrus pars orbitalis, right middle frontal gyrus, right lingual gyrus, right superior frontal gyrus, right dorsal posterior insula, bilateral transverse temporal gyri, and bilateral postcentral gyrus. During the tonic pain state FC from the RPBN ($R > 0.12$) was greater and more extensive on average and included several new regions (Supplemental Fig. 5B). New regions of FC included left inferior occipital gyrus, left inferior frontal gyrus pars orbitalis, left cuneus and calcarine gyrus, left parietal operculum, left superior frontal gyrus, right middle frontal gyrus, left inferior semilunar lobule of the cerebellum, right aMCC, right medial and lateral postcentral gyrus, right inferior frontal gyrus, right paracentral lobule, right cerebellar culmen, bilateral medial dorsal thalamus (Supplemental Table 6).

PAG seed-driven FC ($R > 0.12$) during the pain-free state was consistent with previously published FCNs of the PAG including the sACC, medial thalamus, bilateral lingual gyri, bilateral cerebellar declive and bilateral caudal pons (Supplemental Fig. 6A and Supplemental Table 7) (Kong et al., 2010; Yu et al., 2014). During the tonic pain state PAG seed-driven FC included additional brain regions including aMCC, left paracentral lobule, left postcentral gyrus and rostral ventromedial medulla (Supplemental Fig. 6B and Supplemental Table 8).

Seed-driven FC during the pain-free state from the LAMYG ($R > 0.20$) was consistent with previous reports including significant FC in the bilateral ventromedial prefrontal cortex, frontal operculum, paracentral lobule, fusiform gyri, postcentral gyri, precentral gyri, hippocampus, dorsal posterior and ventral anterior insula, contralateral (right) amygdala and ipsilateral (left) temporo-occipital junction (Supplemental Fig. 7A and Supplemental Table 9) (Gorka et al., 2018; Kerestes et al., 2017; Roy et al., 2009; Simons et al., 2014). During the tonic pain state, FC was stronger and more extensive from the LAMYG seed to the midcingulate cortex, bilateral anterior and posterior insula, bilateral inferior frontal gyri pars orbitalis, bilateral posterior cingulate cortex, left superior parietal lobule and right superior temporal gyrus (Supplemental Fig. 7B and Supplemental Table 10).

Seed-driven FC during the pain-free state from the RAMYG ($R > 0.20$) was consistent with previous reports and that driven from the LAMYG, excepting additional significant FC in the bilateral superior temporal gyri, temporoparietal junction, middle temporal gyri, contralateral (left) amygdala and selective FC limited to the ipsilateral (right) dorsal posterior insula (Supplemental Fig. 8A and Supplemental Table 11). During the tonic pain state, FC was stronger and more extensive from the RAMYG seed to the bilateral posterior insula, left paracentral lobule, left inferior parietal lobule and right fusiform gyrus (Supplemental Fig. 8B and Supplemental Table 12).

3.4. Whole-brain analysis of resting state functional connectivity: contrast between pain and pain-free states

To determine the statistically significant difference between the seed-derived FC of the resting state maps collected during the pain-free task and prolonged tonic pain, we calculated brain-wide contrast maps (Fig. 4). After cluster extent correction at peak p-value of 0.001, there were no significant contrast results from the PAG or RAMYG seeds. During the tonic pain state, the FC from the LAMYG was significantly greater in left middle frontal gyrus (BA8), left superior frontal gyrus, right precentral gyrus, right middle frontal gyrus and bilateral precuneus (Fig. 4A and Table 2A). During the tonic pain state, the FC from the LPBN was significantly greater in the right precentral gyrus (volume=270 mm^3, max t-stat=4.48, MNI coordinates: $x = 44$, $y = -14$, $z = 47$) (Fig. 4B). During the tonic pain state, the FC from the RPBN was significantly greater in bilateral medial postcentral gyrus (Fig. 4C and Table 2B).

3.5. Whole-brain analysis resting state functional connectivity: pain intensity covariance with seed-based FC

In the pain intensity covariation analysis, after cluster extent correction of 270 mm^3 at peak p-value of 0.001, there were no significant correlations of pain intensity with FC from left or right parabrachial nuclei or the periaqueductal gray during pain-free or tonic pain states. See supplemental results for an exploratory analysis reducing the cluster extent criteria to $p < 0.005$ peak intensity and 540 mm^3 cluster size (Supplemental Figs. 9-11).

Pain intensity was significantly positively correlated with FC between the RAMYG seed during the pain-free state and the right claustrum, temporo-occipitoparietal junction (TOPJ) and calcarine gyrus (Fig. 5A and Table 2C).
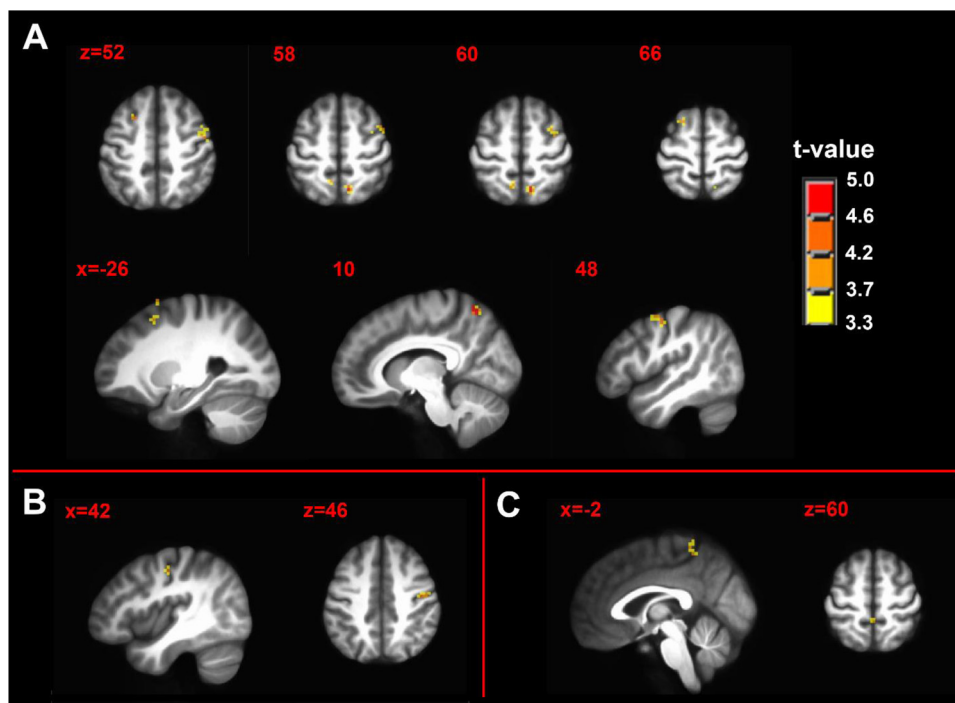
Fig. 4. Contrast maps of tonic pain state > pain-free state of seed-driven functional connectivity from (A) left amygdala complex seed (B) left parabrachial complex seed and (C) right parabrachial complex seed. $n = 50$; minimum cluster size 270 mm³; p-value threshold 0.001. Axial and sagittal labels are in MNI coordinates.

Table 2
Contrast and covariation clusters.

A. Seed: Left Amygdala Test: Pain > Control ($p<0.001$) Cluster Number and Brain Region	Brodmann Area	Volume (mm³)	Maximum Intensity (t-stat)	MNI Coordinates
1. Right Precentral Gyrus	4	810	4.70	(52, −11, 50)
2. Right Precuneus	7	567	5.00	(11, −62, 62)
3. Left Middle Frontal Gyrus	8	324	4.14	(−23, 14, 53)
4. Left Precuneus	7	270	4.06	(−8, −56, 62)
5. Right Middle Frontal Gyrus	6	270	4.01	(35, −5, 62)
6. Left Superior Frontal Gyrus	6	270	4.07	(−20, 14, 71)
B. Seed: Right Parabrachial Nucleus Test: Pain > Control ($p<0.001$)				
1. Right Postcentral Gyrus	5	513	4.84	(11, −44, 71)
2. Left Postcentral Gyrus	5	459	4.31	(−5, −44, 68)
C. Seed: Right Amygdala Test: Correlation with Pain Intensity during Pain-free State ($p<0.001$)				
1. Right Calcarine Gyrus	17	972	4.08	(20, −59, 5)
2. Right Claustrum		405	4.30	(32, 8, −5)
3. Right Temporo-occipitoparietal Junction		270	4.15	(50, −38, 8)
D. Seed: Left Amygdala Test: Correlation with Pain Intensity during Pain State ($p<0.001$)				
1. Right Inferior Temporal Gyrus	20	729	−4.09	(59, −8, −23)

During the tonic pain state, pain intensity was significantly negatively correlated with FC between the LAMYG seed and right inferior temporal gyrus and right superior frontal gyrus (Fig. 5B and Table 2D).

4. Discussion

The purpose of this study was to produce tonic pain via a reliable, interindividually variable model to investigate resting state FC of the DPMN in subcortical brain areas. We operationalized this by hypothesizing specific modulation of FC between several FC dyads including spACC-PAG, pACC-PAG, sACC-PAG, sACC-LPBN, sACC-RPBN, LPBN-PAG, RPBN-PAG, LAMYG-LPBN, and RAMYG-RPBN. Given our limited dyadic FC changes during tonic pain in pain-free participants, we completed exploratory analyses including tests for brain-

wide changes in FC during pain-free and tonic pain states. Finally, we conducted an exploratory analysis covarying pain intensity with brain-wide FC.

4.1. Limited evidence of disruption of node-to-node FC in DPMN

Suprathreshold pain in the C-HP model was robust and highly variable between individuals, inducing robust heat allodynia for at least 75 min (Fig. 2B). Within our hypothesized group of 9 dyads there was only weak evidence of pain disrupting FC between sACC-PAG. In contrast, the effect of sex demonstrated greater pACC-PAG FC in males than females, as previously found in PAG seed-driven FC analyses (Karshikoff et al., 2016). Prior reports of sex differences in FC between ACC and PAG was the driver behind including sex as a factor in our
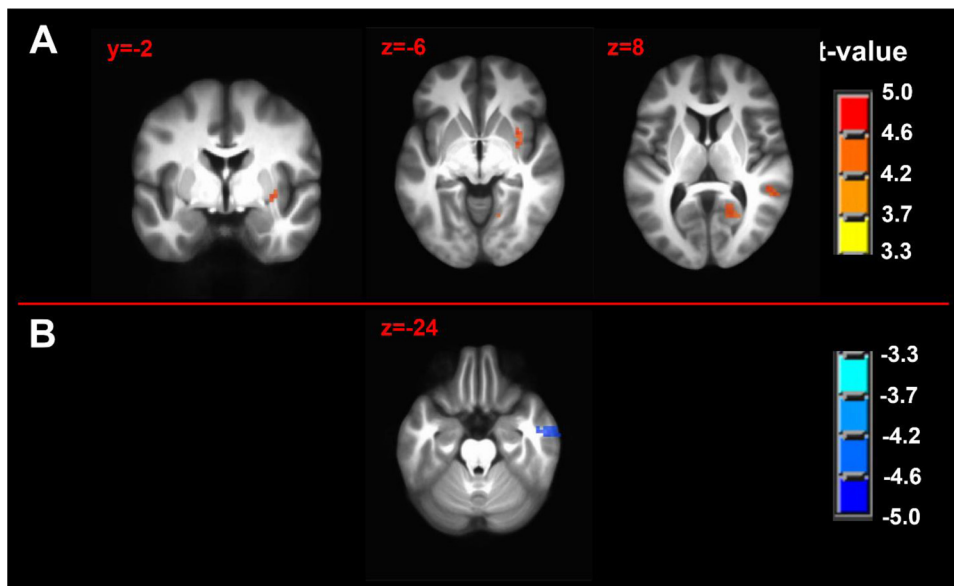
Fig. 5. Pain intensity covariation with seed-driven functional connectivity maps of (A) right amygdala complex seed during pain-free state immediately before and (B) left amygdala complex seed during tonic pain. $n = 50$; minimum cluster size 270 mm³; p-value threshold 0.001. Axial and sagittal labels are in MNI coordinates.

analysis (Tomasi and Volkow, 2012; Wang et al., 2014). For example, increases in brain-wide PAG FC in response to phasic pain are greater in males than female, including with LAMYG. Given the relatively large sample size in this study, failure to find effects of pain in these subcortical connections suggests a relatively weak contribution to the perception of pain.

4.2. FC within the DPMN can predict pain intensity during tonic pain

While the sACC-PAG FC during pain-free rest was unrelated to future pain intensity, it became positively related to pain intensity during tonic pain. Both left and right PBN FC to PAG during pain-free rest were positively related to subsequent pain, but during tonic pain this relationship was no longer significant (Fig. 3B). Pain-free state PBN FC with PAG being associated with pain intensity is supportive of the involvement of this connection in pain regulation in humans, consistent with recent findings in rodent models (Huang et al., 2019; Raver et al., 2020; Roeder et al., 2016).

Our results demonstrate reduction of FC between sACC-PAG by tonic pain, and the first evidence of pain-free PBN-PAG FC being correlated with greater tonic pain experience in humans. It should be noted that our correlational results may support stronger inferences relative to state change results, since our participants experienced pain intensity ranging from just above threshold to severe (75/100 NRS). This variability in pain experience was present with lower exposure temperatures for those participants with greater reported pain intensity and higher exposure temperatures for participants with lower reported pain intensity. This suggests a sensitivity measure of the model may demonstrate a much greater effect in FC compared to pain intensity.

FC and BOLD fMRI modulations associated with pain modulation often include effects in the ACC and PAG. The regions of ACC involved in pain modulation effects associated with PAG include 1) pACC (Coulombe et al., 2016; Eippert et al., 2009; Harper et al., 2018; Kong et al., 2010; Labus et al., 2013; Lee et al., 2021; Leknes et al., 2013; Li et al., 2016; Linnman et al., 2012b; Meeker et al., 2019; Pecina et al., 2015; Peyron et al., 2007; Schmidt-Wilcke et al., 2014; Valet et al., 2004; Wager et al., 2007; Wagner et al., 2001; Wey et al., 2014; Yu et al., 2017, 2014), 2) sACC (Ayoub et al., 2021; Bingel et al., 2006; Labus et al., 2013; Lee et al., 2021; Leknes et al., 2013; Li et al., 2020a; Meeker et al., 2019; Pecina et al., 2015; Schmidt-Wilcke et al., 2014; Sprenger et al., 2011; Wang et al., 2014) or 3) spACC (Atlas et al., 2012; Coulombe et al., 2016; Kong et al., 2010; Lee et al., 2021; Linnman et al., 2012b; Petrovic et al., 2002; Peyron et al., 2007; Rezai et al., 1999;

Schmidt-Wilcke et al., 2014; Schulz et al., 2020; Wager et al., 2007; Wagner et al., 2001). Consistent with these functional reports, non-human primate tractography studies demonstrate afferents projecting to the PAG from pACC and spACC, aMCC, and sACC without reciprocal connections from PAG to cortex (An et al., 1998; Mantyh, 1982b; Porrino and Goldman-Rakic, 1982; Vogt et al., 1987).

4.3. Anatomical evidence of PBN connectivity in animal models and humans

An important spinocortical pathway for nociceptive information from the periphery, most clearly delineated in rodents, which communicates with the DPMN, is the spinoparabrachial pathway (Bernard and Besson, 1990; Gauriau and Bernard, 2002; Polgar et al., 2010; Raver et al., 2020; Roeder et al., 2016). This pathway bypasses the thalamus to project to the cortex directly or via the amygdala and is sensitized by prolonged tonic thermal stimuli (Kissiwaa and Bagley, 2018). In primates, the lateral PBN projects to central nucleus of the amygdala, bed nucleus of the stria terminalis, ventroposteromedial, central lateral, parafascicular/centromedian and reuniens nuclei of the thalamus; dorsomedial, lateral, ventromedial, supramamillary and infundibular nuclei of the hypothalamus; the midbrain PAG, substantia nigra and ventral tegmental area; medullary nucleus ambiguous and reticular formation; and receives a projection from the sACC (Freedman et al., 2000; Pritchard et al., 2000). The primate medial PBN projects to frontal polar cortex, the lateral principal sulcus, medial BA9; and pACC and spACC of the cortex (Porrino and Goldman-Rakic, 1982). Projections from the medial PBN reach the central nucleus of the amygdala; bed nucleus of the stria terminalis; the lateral, dorsal and dorsomedial nuclei of the hypothalamus; ventroposteromedial, central lateral, parafascicular/centromedian and reuniens nuclei of the thalamus; and midbrain PAG and annular nucleus (Pritchard et al., 2000). The lateral and medial parabrachial nuclei are separated by the brachium conjunctivum (Porrino and Goldman-Rakic, 1982). We did not distinguish between lateral and medial PBN in our seeds since we are constrained by low functional resolution and partial volume effects. Relatively few human neuroimaging of studies of the neural correlates of painful stimuli have previously reported PBN activation (Dunckley et al., 2005; Fairhurst et al., 2007; Sprenger et al., 2011; Stroman et al., 2018).

In our FC study of the PBN, we found significant BOLD FC with the caudate, ventral striatum, and medial thalamus subcortically (Supplemental Figs. 4 and 5). Cortically, we found significant BOLD FC with lingual and fusiform gyri, anterior MCC, precentral gyri, transverse tem-

poral gyri, postcentral gyri and anterior and posterior insula. Many of these brain areas likely represent polysynaptic influences of pontine parabrachial complex activity and may aid the PBN complex's role in interoception, pain processing, regulation of food intake and thermoregulation (Benarroch, 2016). Almost the entire pons was included in the cluster of significant FC along with the seed region, obscuring brainstem regions involved in the PBN complex's role in arousal and respiratory control. Importantly, PBN complex FC included areas involved in processing sensory (e.g., primary sensory, posterior insula), affective (e.g., anterior MCC, anterior insula and medial thalamus), and motivational (e.g., BA46, BA9) aspects of pain (Kulkarni et al., 2005; Melzack and Casey, 1968; Rainville et al., 1999a). This multimodal processing capability is consistent with animal studies combining ascending and descending pain processing regions extending rodent model findings to a possible role for the parabrachial complex in pain processing and modulation in humans (Chen and Heinricher, 2019; Kissiwaa and Bagley, 2018; Raver et al., 2020; Roeder et al., 2016; Uddin et al., 2018).

4.4. Modulation of subcortical FC with cortical motor and sensory processing areas

Contrasts between pain-free and pain states of LPBN FC showed enhanced FC to the lateral precentral gyrus in BA4, and from RPBN showed enhanced FC to the medial crown of the postcentral gyrus (Fig. 4B and C). The bilateral medial postcentral gyrus area corresponds to the leg representation of somatosensory cortex, where the painful stimulus was applied. The anterior lateral motor cortex area may be involved in a greater eye-movement or blinking during pain versus pain-free states (Eisenach et al., 2017; Paparella et al., 2020). The LAMYG to whole brain FC contrast demonstrated enhanced FC to the bilateral precuneus, right precentral gyrus, and left middle and superior frontal gyri (Fig. 4A). The significant areas of the BOLD FC changes in the precuneus were in the sensorimotor section with projections to frontal motor control, sensory parietal, and paracentral areas of the brain (Margulies et al., 2009; Morecraft et al., 2004). Enhanced FC from sensorimotor representations of affected body sites to AMYG and PAG are consistent with FC aberrations found in chronic low back pain, chronic neck pain and pressure pain in pain-free participants (Kim et al., 2015, 2013; Kong et al., 2013; Yu et al., 2017, 2014).

Given the variability of reported tonic pain intensity in the MRI scanner environment (range 1–75 out of 100 NRS), we looked for regions of brain-wide FC correlated with pain intensity either during pain-free rest or during tonic pain. During pain-free rest, BOLD FC emanating from the LAMYG to right caudate, right superior parietal lobule and right calcarine gyrus positively correlated with subsequent pain (Supplemental Fig. 7A). This implies cross-hemisphere amygdala FC to higher order sensory cortices is stronger in those individuals more sensitive to pain. This may be related to individual variability in negative affect as recent evidence in pain-free participants showed stronger connectivity of the AMYG to S1/M1, S2/operculum, and posterior parietal cortex at rest in individuals with greater pain facilitation by negative emotions (Gandhi et al., 2020).

4.5. Amygdalocortical FC related to pain intensity during tonic pain

Seed-driven FC from RAMYG to the whole brain was positively associated with subsequent pain intensity experienced during tonic pain specifically in the right visual cortex, right temporo-occipital temporal gyrus and left claustrum (Fig. 5 and Supplemental Fig. 8). Exploratory partial correlation analyses revealed two networks emanating from the RAMYG that related to subsequent tonic pain including 1) RAMYG, right claustrum, and left and right primary visual cortex; and 2) RAMYG, right middle temporal gyrus and right temporo-occipital temporal gyrus (Supplemental Fig. 8). Brain areas in these networks are all highly connected with each other and the rest of the brain, excepting the primary visual cortex (Gorka et al., 2018; Heilbronner and Haber, 2014; Kaas, 2012;

Krimmel et al., 2019; Miyashita et al., 2007). While it may be surprising to observe primary visual cortex implicated in a network correlated with pain intensity, a possible 'vascular steal' effect resulting in decreases in BOLD or blood oxygenation measured by positron emission tomography, in the primary visual cortex by painful stimuli, as well as multisensory processing within the primate visual cortex both have well-established precedent (Coghill et al., 1999; Moulton et al., 2005; Mouraux et al., 2011; Murray et al., 2016).

In exploratory analyses we found seed-driven FC from PAG were positively associated with subsequent pain intensity experienced during tonic pain in right paracentral lobule, RPBN, right medial precuneus, right IPL, left cerebellum, left DLPFC (Supplemental Fig. 9). These regions were interconnected within a PAG-anchored network revealed through partial correlation modeling. Both left DLPFC and right IPL have been implicated in modified pain states, chronic pain states and prediction of chronic pain (Niu et al., 2019; Rainville et al., 1999b; Seminowicz et al., 2018; Seminowicz and Moayedi, 2017; Seminowicz et al., 2011; Symonds et al., 2006). The right paracentral lobule cluster was near the sensory representation of the stimulated left lower leg. Modulation of FC in sensorimotor networks to brainstem and AMYG are consistent with results in both healthy participants experiencing tonic pain and in chronic pain patients (Hubbard et al., 2014; Kim et al., 2015, 2013; Kong et al., 2013; Yu et al., 2014).

4.6. Limitations

It is necessary to point out several limitations of our study. Some of these limitations apply broadly to resting state FC studies, while others are specific. Specific to this study, to achieve reasonable power (0.80) to detect moderate effect sizes ($d = 0.40$; $R = 0.38$), we combined resting state BOLD fMRI datasets acquired with different voxel resolutions (3 mm isotropic vs. $1.8 \times 1.8 \times 4$ mm), did not use white matter signal as a baseline covariate, and used a 4 mm FWHM smoothing kernel. These modifications, some of which were rationalized by adjusting to use of midbrain and pontine seeds, would only decrease the signal-to-noise ratio and, given the sample size, more likely favor the presence of false negatives over false positives taking into account within subject changes (Beissner et al., 2014; Dansereau et al., 2017). Using only motion parameters and motion derivatives regression may be an issue of systematic bias, except that motion outliers, in terms of framewise displacement, were removed; and average framewise displacement was not significantly different between the pain-free and pain state (Parkes et al., 2018). We decided to retain global signal, since global signal regression has biasing effects on long-range FC and introduces negative correlation (Parkes et al., 2018; Saad et al., 2012). Furthermore, non-exploratory primary hypotheses were tested using either manually or atlas-based ROIs or spheres. Since all comparisons are within subject (except for male vs. female contrasts), any significant effects were found with all biases being equal. We clearly did not evaluate all regions or connections which fit our criteria for inclusion in the DPMN as we defined it. We intend to investigate additional regions (e.g., cortical and basal ganglia seeds) in subsequent reports. We must point out that the specific modification we used for the SF-MPQ2 has not been used or validated in studies previously. However, many studies in the past have used a modified version of the original or short form MPQ finding the quality of painful stimuli important (Graven-Nielsen et al., 2002; Harrison and Davis, 1999; Mischkowski et al., 2021; Strigo et al., 2002).

An additional limitation of note is inherent to our study design. Use of the C-HP model in healthy participants made it necessary to perform the pain-free resting state scan before the scan with the tonic heat allodynia produced by the model. This limitation was accepted during the study design for two reasons: 1) exposing the participants to a placebo cream instead of the capsaicin cream during a second randomized ordered scan session was not feasible given the doubling of costs, and 2) we felt an ethical need to expose the participants to the C-HP model outside of the scanner so that subjects would be able to rapidly end the experi-

ment, and be fully informed since some participants found the procedure too painful to endure for 45 min. The lack of counterbalancing order of capsaicin compared to the control condition is not completely overcome by the repeated sessions. For example, it is possible that having the control condition first would increase the salience of the capsaicin during the second session. While the limitation of a fixed order of the scanning sessions clearly applies to the contrast analysis, it is less clear that the correlational results are similarly affected. Importantly, these analyses include participants experiencing a wide range of pain from thermal allodynia with mean ratings ranging from 1 to 75 out of 100 on the VAS. We cannot exclude the possibility that we would not see similar associations in resting state brain activity if participants had, for example, been experiencing, instead of pain, a vibratory or warm stimuli during the resting state condition. Future studies should consider use of comparative paradigms that use extended exposure to salient aversive auditory, tactile, and visual stimulation since brain responses to evoked painful stimuli largely overlap with salient auditory, tactile and visual stimulation (Downar et al., 2003; Legrain et al., 2011; Mouraux et al., 2011).

5. Conclusion

The described pain model induces robust, variable, thermal allodynia allowing a sustained painful state lasting more than 45 min ((Anderson et al., 2002; Meeker et al., 2019) and Fig. 1). We demonstrate 1) of all hypothesized dyads only sACC-PAG FC trended weaker during tonic pain in pain-free healthy participants; 2) sACC-PAG FC during tonic pain positively correlates with self-report pain intensity; 3) RPBN-PAG FC during pain-free rest correlates with subsequent pain intensity during tonic pain and this FC is reduced during tonic pain. Resting state FC of subcortical DPMN-associated structures such the PAG, AMYG and PBN with their cortical targets, as described in this and other recent work, may allow development of novel invasive and non-invasive neuromodulation methods. It is especially relevant to observe these findings in a relatively large sample size of participants in a pathologically relevant human model of nociceptive central sensitization (Lotsch et al., 2014; Meeker et al., 2019, 2021; Quesada et al., 2021; Simone et al., 1991).

Credit authorship contribution statement

Timothy J. Meeker: Conceptualization, Methodology, Formal analysis, Investigation, Visualization, Writing – original draft, Writing – review & editing, Supervision. **Anne-Christine Schmid:** Methodology, Investigation, Writing – original draft, Supervision, Project administration. **Michael L. Keaser:** Methodology, Formal analysis, Investigation, Visualization, Writing – original draft. **Shariq A. Khan:** Investigation, Project administration. **Rao P. Gullapalli:** Methodology, Writing – original draft, Writing – review & editing. **Susan G. Dorsey:** Methodology, Writing – original draft, Writing – review & editing, Supervision, Funding acquisition. **Joel D. Greenspan:** Conceptualization, Methodology, Formal analysis, Writing – original draft, Supervision, Funding acquisition. **David A. Seminowicz:** Conceptualization, Methodology, Formal analysis, Writing – original draft, Writing – review & editing, Supervision, Funding acquisition.

Acknowledgements

Supplementary materials

Supplementary material associated with this article can be found, in the online version, at doi:10.1016/j.neuroimage.2022.119278.

References

An, X., Bandler, R., Ongur, D., Price, J.L., 1998. Prefrontal cortical projections to longitudinal columns in the midbrain periaqueductal gray in macaque monkeys. J. Comp. Neurol. 401, 455–479.

Anderson, W.S., Sheth, R.N., Bencherif, B., Frost, J.J., Campbell, J.N., 2002. Naloxone increases pain induced by topical capsaicin in healthy human volunteers. Pain 99, 207–216.

Atlas, L.Y., Whittington, R.A., Lindquist, M.A., Wielgosz, J., Sonty, N., Wager, T.D., 2012. Dissociable influences of opiates and expectations on pain. J. Neurosci. 32, 8053–8064.

Ayoub, L.J., McAndrews, M.P., Barnett, A.J., Jeremy Ho, K.C., Cioffi, I., Moayedi, M., 2021. Baseline resting-state functional connectivity determines subsequent pain ratings to a tonic ecologically valid experimental model of orofacial pain. Pain 162, 2397–2404 Articles in Press.

Baliki, M.N., Chialvo, D.R., Geha, P.Y., Levy, R.M., Harden, R.N., Parrish, T.B., Apkarian, A.V., 2006. Chronic pain and the emotional brain: specific brain activity associated with spontaneous fluctuations of intensity of chronic back pain. J. Neurosci. 26, 12165–12173.

Baliki, M.N., Petre, B., Torbey, S., Herrmann, K.M., Huang, L., Schnitzer, T.J., Fields, H.L., Apkarian, A.V., 2012. Corticostriatal functional connectivity predicts transition to chronic back pain. Nat. Neurosci. 15, 1117–1119.

Bartoň, M., Mareček, R., Krajčovičová, L., Slavíček, T., Kašpárek, T., Zemánková, P., Říha, P., Mikl, M., 2019. Evaluation of different cerebrospinal fluid and white matter fMRI filtering strategies-quantifying noise removal and neural signal preservation. Hum. Brain Mapp. 40, 1114–1138.

Becerra, L., Morris, S., Bazes, S., Gostic, R., Sherman, S., Gostic, J., Pendse, G., Moulton, E., Scrivani, S., Keith, D., Chizh, B., Borsook, D., 2006. Trigeminal neuropathic pain alters responses in CNS circuits to mechanical (brush) and thermal (cold and heat) stimuli. J. Neurosci. 26, 10646–10657.

Beissner, F., Schumann, A., Brunn, F., Eisentrager, D., Bar, K.J., 2014. Advances in functional magnetic resonance imaging of the human brainstem. Neuroimage 86, 91–98.

Benarroch, E.E., 2016. Parabrachial nuclear complex: multiple functions and potential clinical implications. Neurology 86, 676–683.

Bernard, J.F., Besson, J.M., 1990. The spino(trigemino)pontoamygdaloid pathway: electrophysiological evidence for an involvement in pain processes. J. Neurophysiol. 63, 473–490.

Bingel, U., Lorenz, J., Schoell, E., Weiller, C., Buchel, C., 2006. Mechanisms of placebo analgesia: rACC recruitment of a subcortical antinociceptive network. Pain 120, 8–15.

Biswal, B., Yetkin, F.Z., Haughton, V.M., Hyde, J.S., 1995. Functional connectivity in the motor cortex of resting human brain using echo-planar MRI. Magn. Reson. Med. 34, 537–541.

Bush, G., Shin, L.M., 2006. The Multi-Source Interference Task: an fMRI task that reliably activates the cingulo-frontal-parietal cognitive/attention network. Nat. Protoc. 1, 308–313.

Cavallone, L.F., Frey, K., Montana, M.C., Joyal, J., Regina, K.J., Petersen, K.L., Gereau, R.W.t., 2013. Reproducibility of the heat/capsaicin skin sensitization model in healthy volunteers. J. Pain Res. 6, 771–784.

Chen, A.C.N., Treede, R.D., 1985. The McGill Pain Questionnaire in the assessment of phasic and tonic experimental pain: behavioral evaluation of the 'pain inhibiting pain' effect. Pain 22, 67–79.

Chen, G., Saad, Z.S., Britton, J.C., Pine, D.S., Cox, R.W., 2013. Linear mixed-effects modeling approach to FMRI group analysis. Neuroimage 73, 176–190.

Chen, Q., Heinricher, M.M., 2019. Plasticity in the link between pain-transmitting and pain-modulating systems in acute and persistent inflammation. J. Neurosci. 39, 2065–2079.

Coghill, R.C., Sang, C.N., Maisog, J.M., Iadarola, M.J., 1999. Pain intensity processing within the human brain: a bilateral, distributed mechanism. J. Neurophysiol. 82, 1934–1943.

Coulombe, M.A., Erpelding, N., Kucyi, A., Davis, K.D., 2016. Intrinsic functional connectivity of periaqueductal gray subregions in humans. Hum. Brain Mapp. 37, 1514–1530.

Crockett, D.J., Prkachin, K.M., Craig, K.D., 1977. Factors of the language of pain in patient and volunteer groups. Pain 4, 175–182.

Crowther, A., Smoski, M.J., Minkel, J., Moore, T., Gibbs, D., Petty, C., Bizzell, J., Schiller, C.E., Sideris, J., Carl, H., Dichter, G.S., 2015. Resting-state connectivity predictors of response to psychotherapy in major depressive disorder. Neuropsychopharmacology 40, 1659–1673.

Dansereau, C., Benhajali, Y., Risterucci, C., Pich, E.M., Orban, P., Arnold, D., Bellec, P., 2017. Statistical power and prediction accuracy in multisite resting-state fMRI connectivity. Neuroimage 149, 220–232.

deCharms, R.C., Maeda, F., Glover, G.H., Ludlow, D., Pauly, J.M., Soneji, D., Gabrieli, J.D., Mackey, S.C., 2005. Control over brain activation and pain learned by using real-time functional MRI. Proc. Natl. Acad. Sci. U. S. A. 102, 18626–18631.

Downar, J., Mikulis, D.J., Davis, K.D., 2003. Neural correlates of the prolonged salience of painful stimulation. Neuroimage 20, 1540–1551.

Dunckley, P., Wise, R.G., Fairhurst, M., Hobden, P., Aziz, Q., Chang, L., Tracey, I., 2005. A comparison of visceral and somatic pain processing in the human brainstem using functional magnetic resonance imaging. J. Neurosci. 25, 7333–7341.

Dworkin, R.H., Turk, D.C., Revicki, D.A., Harding, G., Coyne, K.S., Peirce-Sandner, S., Bhagwat, D., Everton, D., Burke, L.B., Cowan, P., Farrar, J.T., Hertz, S., Max, M.B., Rappaport, B.A., Melzack, R., 2009. Development and initial validation of an expanded and revised version of the short-form McGill pain questionnaire (SF-MPQ-2). Pain 144, 35–42.

Eippert, F., Bingel, U., Schoell, E.D., Yacubian, J., Klinger, R., Lorenz, J., Buchel, C., 2009. Activation of the opioidergic descending pain control system underlies placebo analgesia. Neuron 63, 533–543.

Eisenach, J.C., Curry, R., Aschenbrenner, C.A., Coghill, R.C., Houle, T.T., 2017. Pupil responses and pain ratings to heat stimuli: reliability and effects of expectations and a conditioning pain stimulus. J. Neurosci. Methods 279, 52–59.

Fairhurst, M., Wiech, K., Dunckley, P., Tracey, I., 2007. Anticipatory brainstem activity predicts neural processing of pain in humans. Pain 128, 101–110.

Fisher, R.A., 1948. Statistical Methods FOR Research Workers. Oliver and Boyd, Edinburgh [etc.].

Foss, J.M., Apkarian, A.V., Chialvo, D.R., 2006. Dynamics of pain: fractal dimension of temporal variability of spontaneous pain differentiates between pain States. J. Neurophysiol. 95, 730–736.

Freedman, L.J., Insel, T.R., Smith, Y., 2000. Subcortical projections of area 25 (subgenual cortex) of the macaque monkey. J. Comp. Neurol. 421, 172–188.

Gandhi, W., Rosenek, N.R., Harrison, R., Salomons, T.V., 2020. Functional connectivity of the amygdala is linked to individual differences in emotional pain facilitation. Pain 161, 300–307.

Garcia-Larrea, L., Peyron, R., 2007. Motor cortex stimulation for neuropathic pain: from phenomenology to mechanisms. Neuroimage 37 (Suppl 1), S71–S79.

Gauriau, C., Bernard, J.F., 2002. Pain pathways and parabrachial circuits in the rat. Exp. Physiol. 87, 251–258.

Gorka, A.X., Torrisi, S., Shackman, A.J., Grillon, C., Ernst, M., 2018. Intrinsic functional connectivity of the central nucleus of the amygdala and bed nucleus of the stria terminalis. Neuroimage 168, 392–402.

Graven-Nielsen, T., Arendt-Nielsen, L., Mense, S., 2002. Thermosensitivity of muscle: high-intensity thermal stimulation of muscle tissue induces muscle pain in humans. J. Physiol. 540, 647–656.

Green, B.G., Flammer, L.J., 1988. Capsaicin as a cutaneous stimulus: sensitivity and sensory qualities on hairy skin. Chem. Sens. 13, 367–384.

Greenspan, J.D., 2013. Threshold Determination Methods. Encyclopedia of Pain. Springer, Berlin Heidelberg.

Greenspan, J.D., Roy, E.A., Caldwell, P.A., Farooq, N.S., 2003. Thermosensory intensity and affect throughout the perceptible range. Somatosens. Mot. Res. 20, 19–26.

Harper, D.E., Ichesco, E., Schrepf, A., Hampson, J.P., Clauw, D.J., Schmidt-Wilcke, T., Harris, R.E., Harte, S.E., 2018. Resting functional connectivity of the periaqueductal gray is associated with normal inhibition and pathological facilitation in conditioned pain modulation. J. Pain 19, 635.e1–635.e15.

Harrison, J.L., Davis, K.D., 1999. Cold-evoked pain varies with skin type and cooling rate: a psychophysical study in humans. Pain 83, 123–135.

Heilbronner, S.R., Haber, S.N., 2014. Frontal cortical and subcortical projections provide a basis for segmenting the cingulum bundle: implications for neuroimaging and psychiatric disorders. J Neurosci 34, 10041–10054.

Henriksen, G., Willoch, F., 2008. Imaging of opioid receptors in the central nervous system. Brain 131, 1171–1196.

Huang, T., Lin, S.H., Malewicz, N.M., Zhang, Y., Zhang, Y., Goulding, M., LaMotte, R.H., Ma, Q., 2019. Identifying the pathways required for coping behaviours associated with sustained pain. Nature 565, 86–90.

Hubbard, C.S., Khan, S.A., Keaser, M.L., Mathur, V.A., Goyal, M., Seminowicz, D.A., 2014. Altered Brain Structure and Function Correlate with Disease Severity and Pain Catastrophizing in Migraine Patients. eNeuro 5 ENEURO.0354-17.2018.

Jo, H.J., Saad, Z.S., Simmons, W.K., Milbury, L.A., Cox, R.W., 2010. Mapping sources of correlation in resting state FMRI, with artifact detection and removal. Neuroimage 52, 571–582.

Kaas, J.H., 2012. The evolution of neocortex in primates. Prog. Brain Res. 195, 91–102.

Karshikoff, B., Jensen, K.B., Kosek, E., Kalpouzos, G., Soop, A., Ingvar, M., Olgart Hoglund, C., Lekander, M., Axelsson, J., 2016. Why sickness hurts: a central mechanism for pain induced by peripheral inflammation. Brain Behav. Immun. 57, 38–46.

Ke, J., Qi, R., Liu, C., Xu, Q., Wang, F., Zhang, L., Lu, G., 2015. Abnormal regional homogeneity in patients with irritable bowel syndrome: a resting-state functional MRI study. Neurogastroenterol. Motil. 27, 1796–1803.

Kerestes, R., Chase, H.W., Phillips, M.L., Ladouceur, C.D., Eickhoff, S.B., 2017. Multimodal evaluation of the amygdala's functional connectivity. Neuroimage 148, 219–229.

Khalili-Mahani, N., Rombouts, S.A., van Osch, M.J., Duff, E.P., Carbonell, F., Nickerson, L.D., Becerra, L., Dahan, A., Evans, A.C., Soucy, J.P., Wise, R., Zijdenbos, A.P., van Gerven, J.M., 2017. Biomarkers, designs, and interpretations of resting-state fMRI in translational pharmacological research: a review of state-of-the-Art, challenges, and opportunities for studying brain chemistry. Hum. Brain Mapp. 38, 2276–2325.

Kim, J., Loggia, M.L., Cahalan, C.M., Harris, R.E., Beissner, F.D.P.N., Garcia, R.G., Kim, H., Wasan, A.D., Edwards, R.R., Napadow, V., 2015. The somatosensory link in fibromyalgia: functional connectivity of the primary somatosensory cortex is altered by sustained pain and is associated with clinical/autonomic dysfunction. Arthritis Rheumatol. 67, 1395–1405.

Kim, J., Loggia, M.L., Edwards, R.R., Wasan, A.D., Gollub, R.L., Napadow, V., 2013. Sustained deep-tissue pain alters functional brain connectivity. Pain 154, 1343–1351.

Kissiwaa, S.A., Bagley, E.E., 2018. Central sensitization of the spino-parabrachial-amygdala pathway that outlasts a brief nociceptive stimulus. J. Physiol. 596, 4457–4473.

Klepac, R.K., Dowling, J., Hauge, G., 1981. Sensitivity of the McGill pain questionnaire to intensity and quality of laboratory pain. Pain 10, 199–207.

Koenig, J., Jarczok, M.N., Ellis, R.J., Bach, C., Thayer, J.F., Hillecke, T.K., 2014. Two-week test-retest stability of the cold pressor task procedure at two different temperatures as a measure of pain threshold and tolerance. Pain Practice 14, E126–E135.

Kong, J., Spaeth, R.B., Wey, H.Y., Cheetham, A., Cook, A.H., Jensen, K., Tan, Y., Liu, H., Wang, D., Loggia, M.L., Napadow, V., Smoller, J.W., Wasan, A.D., Gollub, R.L., 2013. S1 is associated with chronic low back pain: a functional and structural MRI study. Mol. Pain 9, 43.

Kong, J., Tu, P.C., Zyloney, C., Su, T.P., 2010. Intrinsic functional connectivity of the periaqueductal gray, a resting fMRI study. Behav. Brain Res. 211, 215–219.

Krimmel, S.R., White, M.G., Panicker, M.H., Barrett, F.S., Mathur, B.N., Seminowicz, D.A., 2019. Resting state functional connectivity and cognitive task-related activation of the human claustrum. Neuroimage 196, 59–67.

Kucyi, A., Salomons, T.V., Davis, K.D., 2013. Mind wandering away from pain dynamically engages antinociceptive and default mode brain networks. Proc. Natl. Acad. Sci. U. S. A. 110, 18692–18697.

Kulkarni, B., Bentley, D.E., Elliott, R., Youell, P., Watson, A., Derbyshire, S.W., Frackowiak, R.S., Friston, K.J., Jones, A.K., 2005. Attention to pain localization and unpleasantness discriminates the functions of the medial and lateral pain systems. Eur. J. Neurosci. 21, 3133–3142.

Labus, J.S., Hubbard, C.S., Bueller, J., Ebrat, B., Tillisch, K., Chen, M., Stains, J., Dukes, G.E., Kelleher, D.L., Naliboff, B.D., Fanselow, M., Mayer, E.A., 2013. Impaired emotional learning and involvement of the corticotropin-releasing factor signaling system in patients with irritable bowel syndrome. Gastroenterology 145 1253-61.e1-3.

Lakens, D., 2013. Calculating and reporting effect sizes to facilitate cumulative science: a practical primer for t-tests and ANOVAs. Front. Psychol. 4, 863.

Lee, J.J., Kim, H.J., Čeko, M., Park, B.Y., Lee, S.A., Park, H., Roy, M., Kim, S.G., Wager, T.D., Woo, C.W., 2021. A neuroimaging biomarker for sustained experimental and clinical pain. Nat. Med. 27, 174–182.

Legrain, V., Iannetti, G.D., Plaghki, L., Mouraux, A., 2011. The pain matrix reloaded: a salience detection system for the body. Prog. Neurobiol. 93, 111–124.

Leknes, S., Berna, C., Lee, M.C., Snyder, G.D., Biele, G., Tracey, I., 2013. The importance of context: when relative relief renders pain pleasant. Pain 154, 402–410.

Li, H., Li, X., Feng, Y., Gao, F., Kong, Y., Hu, L., 2020a. Deficits in ascending and descending pain modulation pathways in patients with postherpetic neuralgia. Neuroimage 221, 117186.

Li, M., Gao, Y., Gao, F., Anderson, A.W., Ding, Z., Gore, J.C., 2020b. Functional engagement of white matter in resting-state brain networks. Neuroimage 220, 117096.

Li, Z., Zhao, L., Liu, M., Lan, L., Zeng, F., Makris, N., Liang, Y., Guo, T., Wu, F., Gao, Y., Dong, M., Yang, J., Li, Y., Gong, Q., Liang, F., Kong, J., 2016. Altered periaqueductal gray resting state functional connectivity in migraine and the modulation effect of treatment. Sci. Rep. 6, 20298.

Linnman, C., Beucke, J.C., Jensen, K.B., Gollub, R.L., Kong, J., 2012a. Sex similarities and differences in pain-related periaqueductal gray connectivity. Pain 153, 444–454.

Linnman, C., Moulton, E.A., Barmettler, G., Becerra, L., Borsook, D., 2012b. Neuroimaging of the periaqueductal gray: state of the field. Neuroimage 60, 505–522.

Liu, J., Zhao, L., Li, G., Xiong, S., Nan, J., Li, J., Yuan, K., von Deneen, K.M., Liang, F., Qin, W., Tian, J., 2012. Hierarchical alteration of brain structural and functional networks in female migraine sufferers. PLoS ONE 7, e51250.

Liu, M., Max, M.B., Robinovitz, E., Gracely, R.H., Bennett, G.J., 1998. The human capsaicin model of allodynia and hyperalgesia: sources of variability and methods for reduction. J. Pain Symptom Manage. 16, 10–20.

Lotsch, J., Oertel, B.G., Ultsch, A., 2014. Human models of pain for the prediction of clinical analgesia. Pain 155, 2014–2021.

Luke, S.G., 2017. Evaluating significance in linear mixed-effects models in R. Behav. Res. Methods 49, 1494–1502.

Mantyh, P.W., 1982a. The ascending input to the midbrain periaqueductal gray of the primate. J. Comp. Neurol. 211, 50–64.

Mantyh, P.W., 1982b. Forebrain projections to the periaqueductal gray in the monkey, with observations in the cat and rat. J. Comp. Neurol. 206, 146–158.

Mantyh, P.W., 1983. Connections of midbrain periaqueductal gray in the monkey. II. Descending efferent projections. J. Neurophysiol. 49, 582–594.

Margulies, D.S., Vincent, J.L., Kelly, C., Lohmann, G., Uddin, L.Q., Biswal, B.B., Villringer, A., Castellanos, F.X., Milham, M.P., Petrides, M., 2009. Precuneus shares intrinsic functional architecture in humans and monkeys. Proc. Natl. Acad. Sci. U. S. A. 106, 20069–20074.

Meeker, T.J., Keaser, M.L., Khan, S.A., Gullapalli, R.P., Seminowicz, D.A., Greenspan, J.D., 2019. Non-invasive motor cortex neuromodulation reduces secondary hyperalgesia and enhances activation of the descending pain modulatory network. Front. Neurosci. 13, 18.

Meeker, T.J., Schmid, A.C., Liu, Y., Keaser, M.L., Dorsey, S.G., Seminowicz, D.A., Greenspan, J.D., 2021. During capsaicin-induced central sensitization, brush allodynia is associated with baseline warmth sensitivity, whereas mechanical hyperalgesia is associated with painful mechanical sensibility, anxiety and somatization. Eur. J. Pain 25, 1971–1993.

Melzack, R., Casey, K.L., 1968. Sensory, motivational, and central control determinants of pain: a new conceptual model. In: Kenshalo, D.R. (Ed.), The Skin Senses: Proceedings of the First International Symposium on the Skin Senses. Charles C. Thomas, Springfield, Illinois, p. 636.

Mischkowski, D., Stavish, C.M., Palacios-Barrios, E.E., Banker, L.A., Dildine, T.C., Atlas, L.Y., 2021. Dispositional mindfulness and acute heat pain: comparing stimulus-evoked pain with summary pain assessment. Psychosom. Med. 83, 539–548.

Mishra, A., Li, M., Anderson, A.W., Newton, A.T., Ding, Z., Gore, J.C., 2020. Concomitant modulation of BOLD responses in white matter pathways and cortex. Neuroimage 216, 116791.

Miyashita, T., Ichinohe, N., Rockland, K.S., 2007. Differential modes of termination of amygdalothalamic and amygdalocortical projections in the monkey. J. Comp. Neurol. 502, 309–324.

Morecraft, R.J., Cipolloni, P.B., Stilwell-Morecraft, K.S., Gedney, M.T., Pandya, D.N., 2004. Cytoarchitecture and cortical connections of the posterior cingulate and adjacent somatosensory fields in the rhesus monkey. J. Comp. Neurol. 469, 37–69.

2nd Morey, R.A., Petty, C.M., Xu, Y., Hayes, J.P., Wagner, H.R., Lewis, D.V., LaBar, K.S., Styner, M., McCarthy, G., 2009. A comparison of automated segmentation and manual tracing for quantifying hippocampal and amygdala volumes. Neuroimage 45, 855–866.

Moritz, A.R., Henriques, F.C., 1947. Studies of thermal injury: II. The relative importance of time and surface temperature in the causation of cutaneous burns. Am. J. Pathol. 23, 695–720.

Moulton, E.A., Keaser, M.L., Gullapalli, R.P., Greenspan, J.D., 2005. Regional intensive and temporal patterns of functional MRI activation distinguishing noxious and innocuous contact heat. J. Neurophysiol. 93, 2183–2193.

Moulton, E.A., Pendse, G., Morris, S., Strassman, A., Aiello-Lammens, M., Becerra, L., Borsook, D., 2007. Capsaicin-induced thermal hyperalgesia and sensitization in the human trigeminal nociceptive pathway: an fMRI study. Neuroimage 35, 1586–1600.

Mouraux, A., Diukova, A., Lee, M.C., Wise, R.G., Iannetti, G.D., 2011. A multisensory investigation of the functional significance of the "pain matrix". Neuroimage 54, 2237–2249.

Murray, M.M., Thelen, A., Thut, G., Romei, V., Martuzzi, R., Matusz, P.J., 2016. The multisensory function of the human primary visual cortex. Neuropsychologia 83, 161–169.

Niu, X., Bai, L., Sun, Y., Wang, S., Cao, J., Sun, C., Wang, Z., Xu, H., Gan, S., Fan, G., Huang, W., Gu, C., Yin, B., Bai, G., Xu, X., Zhang, M., 2019. Disruption of periaqueductal grey-default mode network functional connectivity predicts persistent post–traumatic headache in mild traumatic brain injury. J. Neurol. Neurosurg. Psychiatry 90, 326–332.

Oldfield, R.C., 1971. The assessment and analysis of handedness: the Edinburgh inventory. Neuropsychologia 9, 97–113.

Paparella, G., Di Stefano, G., Fasolino, A., Di Pietro, G., Colella, D., Truini, A., Cruccu, G., Berardelli, A., Bologna, M., 2020. Painful stimulation increases spontaneous blink rate in healthy subjects. Sci. Rep. 10, 20014.

Parkes, L., Fulcher, B., Yücel, M., Fornito, A., 2018. An evaluation of the efficacy, reliability, and sensitivity of motion correction strategies for resting-state functional MRI. Neuroimage 171, 415–436.

Pecina, M., Love, T., Stohler, C.S., Goldman, D., Zubieta, J.K., 2015. Effects of the Mu opioid receptor polymorphism (OPRM1 A118G) on pain regulation, placebo effects and associated personality trait measures. Neuropsychopharmacology 40, 957–965.

Peer, M., Nitzan, M., Bick, A.S., Levin, N., Arzy, S., 2017. Evidence for functional networks within the human brain's white matter. J. Neurosci. 37, 6394–6407.

Petersen, K.L., Rowbotham, M.C., 1999. A new human experimental pain model: the heat/capsaicin sensitization model. NeuroReport 10, 1511–1516.

Petrovic, P., Kalso, E., Petersson, K.M., Ingvar, M., 2002. Placebo and opioid analgesia–imaging a shared neuronal network. Science 295, 1737–1740.

Peyron, R., Faillenot, I., Mertens, P., Laurent, B., Garcia-Larrea, L., 2007. Motor cortex stimulation in neuropathic pain. Correlations between analgesic effect and hemodynamic changes in the brain. A PET study. Neuroimage 34, 310–321.

Polgar, E., Wright, L.L., Todd, A.J., 2010. A quantitative study of brainstem projections from lamina I neurons in the cervical and lumbar enlargement of the rat. Brain Res. 1308, 58–67.

Porrino, L.J., Goldman-Rakic, P.S., 1982. Brainstem innervation of prefrontal and anterior cingulate cortex in the rhesus monkey revealed by retrograde transport of HRP. J. Comp. Neurol. 205, 63–76.

Price, R.C., Gandhi, W., Nadeau, C., Tarnavskiy, R., Qu, A., Fahey, E., Stone, L., Schweinhardt, P., 2018. Characterization of a novel capsaicin/heat ongoing pain model. Eur. J. Pain 22, 370–384.

Pritchard, T.C., Hamilton, R.B., Norgren, R., 2000. Projections of the parabrachial nucleus in the old world monkey. Exp. Neurol. 165, 101–117.

Quesada, C., Kostenko, A., Ho, I., Leone, C., Nochi, Z., Stouffs, A., Wittayer, M., Caspani, O., Brix Finnerup, N., Mouraux, A., Pickering, G., Tracey, I., Truini, A., Treede, R.D., Garcia-Larrea, L., 2021. Human surrogate models of central sensitization: a critical review and practical guide. Eur. J. Pain 25, 1389–1428.

Raichle, M.E., MacLeod, A.M., Snyder, A.Z., Powers, W.J., Gusnard, D.A., Shulman, G.L., 2001. A default mode of brain function. Proc. Natl. Acad. Sci. U. S. A. 98, 676–682.

Rainville, P., Carrier, B., Hofbauer, R.K., Bushnell, C.M., Duncan, G.H., 1999a. Dissociation of sensory and affective dimensions of pain using hypnotic modulation. Pain 82, 159–171.

Rainville, P., Hofbauer, R.K., Paus, T., Duncan, G.H., Bushnell, M.C., Price, D.D., 1999b. Cerebral mechanisms of hypnotic induction and suggestion. J Cogn. Neurosci. 11, 110–125.

Raver, C., Uddin, O., Ji, Y., Li, Y., Cramer, N., Jenne, C., Morales, M., Masri, R., Keller, A., 2020. An Amygdalo-parabrachial pathway regulates pain perception and chronic pain. J. Neurosci. 40, 3424–3442.

Rezai, A.R., Lozano, A.M., Crawley, A.P., Joy, M.L., Davis, K.D., Kwan, C.L., Dostrovsky, J.O., Tasker, R.R., Mikulis, D.J., 1999. Thalamic stimulation and functional magnetic resonance imaging: localization of cortical and subcortical activation with implanted electrodes. Technical note. J. Neurosurg. 90, 583–590.

Roeder, Z., Chen, Q., Davis, S., Carlson, J.D., Tupone, D., Heinricher, M.M., 2016. Parabrachial complex links pain transmission to descending pain modulation. Pain 157, 2697–2708.

Roy, A.K., Shehzad, Z., Margulies, D.S., Kelly, A.M., Uddin, L.Q., Gotimer, K., Biswal, B.B., Castellanos, F.X., Milham, M.P., 2009. Functional connectivity of the human amygdala using resting state fMRI. Neuroimage 45, 614–626.

Saad, Z.S., Gotts, S.J., Murphy, K., Chen, G., Jo, H.J., Martin, A., Cox, R.W., 2012. Trouble at rest: how correlation patterns and group differences become distorted after global signal regression. Brain Connect 2, 25–32.

Schmidt-Wilcke, T., Ichesco, E., Hampson, J.P., Kairys, A., Peltier, S., Harte, S., Clauw, D.J., 2014. Resting state connectivity correlates with drug and placebo response in fibromyalgia patients. NeuroImage 6, 252–261.

Schulz, E., Stankewitz, A., Winkler, A.M., Irving, S., Witkovsky, V., Tracey, I., 2020. Ultra-high-field imaging reveals increased whole brain connectivity underpins cognitive strategies that attenuate pain. Elife 9, e55028.

Seminowicz, D.A., Davis, K.D., 2007. Pain enhances functional connectivity of a brain network evoked by performance of a cognitive task. J Neurophysiol 97, 3651–3659.

Seminowicz, D.A., de Martino, E., Schabrun, S.M., Graven-Nielsen, T., 2018. Left dorsolateral prefrontal cortex repetitive transcranial magnetic stimulation reduces the development of long-term muscle pain. Pain 159, 2486–2492.

Seminowicz, D.A., Moayedi, M., 2017. The dorsolateral prefrontal cortex in acute and chronic pain. J. Pain 18, 1027–1035.

Seminowicz, D.A., Wideman, T.H., Naso, L., Hatami-Khoroushahi, Z., Fallatah, S., Ware, M.A., Jarzem, P., Bushnell, M.C., Shir, Y., Ouellet, J.A., Stone, L.S., 2011. Effective treatment of chronic low back pain in humans reverses abnormal brain anatomy and function. J. Neurosci. 31, 7540–7550.

Seymour, B., O'Doherty, J.P., Koltzenburg, M., Wiech, K., Frackowiak, R., Friston, K., Dolan, R., 2005. Opponent appetitive-aversive neural processes underlie predictive learning of pain relief. Nat. Neurosci. 8, 1234–1240.

Simone, D.A., Sorkin, L.S., Oh, U., Chung, J.M., Owens, C., LaMotte, R.H., Willis, W.D., 1991. Neurogenic hyperalgesia: central neural correlates in responses of spinothalamic tract neurons. J. Neurophysiol. 66, 228–246.

Simons, L.E., Pielech, M., Erpelding, N., Linnman, C., Moulton, E., Sava, S., Lebel, A., Serrano, P., Sethna, N., Berde, C., Becerra, L., Borsook, D., 2014. The responsive amygdala: treatment-induced alterations in functional connectivity in pediatric complex regional pain syndrome. Pain 155, 1727–1742.

Sprenger, C., Bingel, U., Buchel, C., 2011. Treating pain with pain: supraspinal mechanisms of endogenous analgesia elicited by heterotopic noxious conditioning stimulation. Pain 152, 428–439.

Stohler, C.S., Kowalski, C.J., 1999. Spatial and temporal summation of sensory and affective dimensions of deep somatic pain. Pain 79, 165–173.

Strigo, I.A., Bushnell, C.M., Boivin, M., Duncan, G.H., 2002. Psychophysical analysis of visceral and cutaneous pain in human subjects. Pain 97, 235–246.

Stroman, P.W., Ioachim, G., Powers, J.M., Staud, R., Pukall, C., 2018. Pain processing in the human brainstem and spinal cord before, during, and after the application of noxious heat stimuli. Pain 159, 2012–2020.

Symonds, L.L., Gordon, N.S., Bixby, J.C., Mande, M.M., 2006. Right-lateralized pain processing in the human cortex: an FMRI study. J. Neurophysiol. 95, 3823–3830.

Tomasi, D., Volkow, N.D., 2012. Gender differences in brain functional connectivity density. Hum. Brain Mapp. 33, 849–860.

Uddin, O., Studlack, P., Akintola, T., Raver, C., Castro, A., Masri, R., Keller, A., 2018. Amplified parabrachial nucleus activity in a rat model of trigeminal neuropathic pain. Neurobiol. Pain 3, 22–30.

Valet, M., Sprenger, T., Boecker, H., Willoch, F., Rummeny, E., Conrad, B., Erhard, P., Tolle, T.R., 2004. Distraction modulates connectivity of the cingulo-frontal cortex and the midbrain during pain–an fMRI analysis. Pain 109, 399–408.

Vogt, B.A., Pandya, D.N., Rosene, D.L., 1987. Cingulate cortex of the rhesus monkey: I. Cytoarchitecture and thalamic afferents. J. Comp. Neurol. 262, 256–270.

Vos de Wael, R., Hyder, F., Thompson, G.J., 2017. Effects of tissue-specific functional magnetic resonance imaging signal regression on resting-state functional connectivity. Brain Connect 7, 482–490.

Wager, T.D., Scott, D.J., Zubieta, J.K., 2007. Placebo effects on human mu-opioid activity during pain. Proc. Natl. Acad. Sci. U. S. A. 104, 11056–11061.

Wagner, K.J., Willoch, F., Kochs, E.F., Siessmeier, T., Tölle, T.R., Schwaiger, M., Bartenstein, P., 2001. Dose-dependent regional cerebral blood flow changes during remifentanil infusion in humans: a positron emission tomography study. Anesthesiology 94, 732–739.

Walsh, D.M., Liggett, C., Baxter, D., Allen, J.M., 1995. A double-blind investigation of the hypoalgesic effects of transcutaneous electrical nerve stimulation upon experimentally induced ischaemic pain. Pain 61, 39–45.

Wang, G., Erpelding, N., Davis, K.D., 2014. Sex differences in connectivity of the subgenual anterior cingulate cortex. Pain 155, 755–763.

Wasserstein, R.L., Lazar, N.A., 2016. The ASA's statement onp-values: context, process, and purpose. Am. Stat. 70, 129–133.

Wei, S.Y., Chao, H.T., Tu, C.H., Li, W.C., Low, I., Chuang, C.Y., Chen, L.F., Hsieh, J.C., 2016. Changes in functional connectivity of pain modulatory systems in women with primary dysmenorrhea. Pain 157, 92–102.

Wey, H.Y., Catana, C., Hooker, J.M., Dougherty, D.D., Knudsen, G.M., Wang, D.J.J., Chonde, D.B., Rosen, B.R., Gollub, R.L., Kong, J., 2014. Simultaneous fMRI-PET of the opioidergic pain system in human brain. Neuroimage 102, 275–282.

Wiech, K., Seymour, B., Kalisch, R., Stephan, K.E., Koltzenburg, M., Driver, J., Dolan, R.J., 2005. Modulation of pain processing in hyperalgesia by cognitive demand. Neuroimage 27, 59–69.

Wu, T.H., Tu, C.H., Chao, H.T., Li, W.C., Low, I., Chuang, C.Y., Yeh, T.C., Cheng, C.M., Chou, C.C., Chen, L.F., Hsieh, J.C., 2016. Dynamic changes of functional pain connectome in women with primary dysmenorrhea. Sci. Rep. 6, 24543.

Yu, C.X., Li, B., Xu, Y.K., Ji, T.T., Li, L., Zhao, C.J., Chen, L., Zhuo, Z.Z., 2017. Altered functional connectivity of the periaqueductal gray in chronic neck and shoulder pain. NeuroReport 28, 720–725.

Yu, R., Gollub, R.L., Spaeth, R., Napadow, V., Wasan, A., Kong, J., 2014. Disrupted functional connectivity of the periaqueductal gray in chronic low back pain. Neuroimage Clin. 6, 100–108.